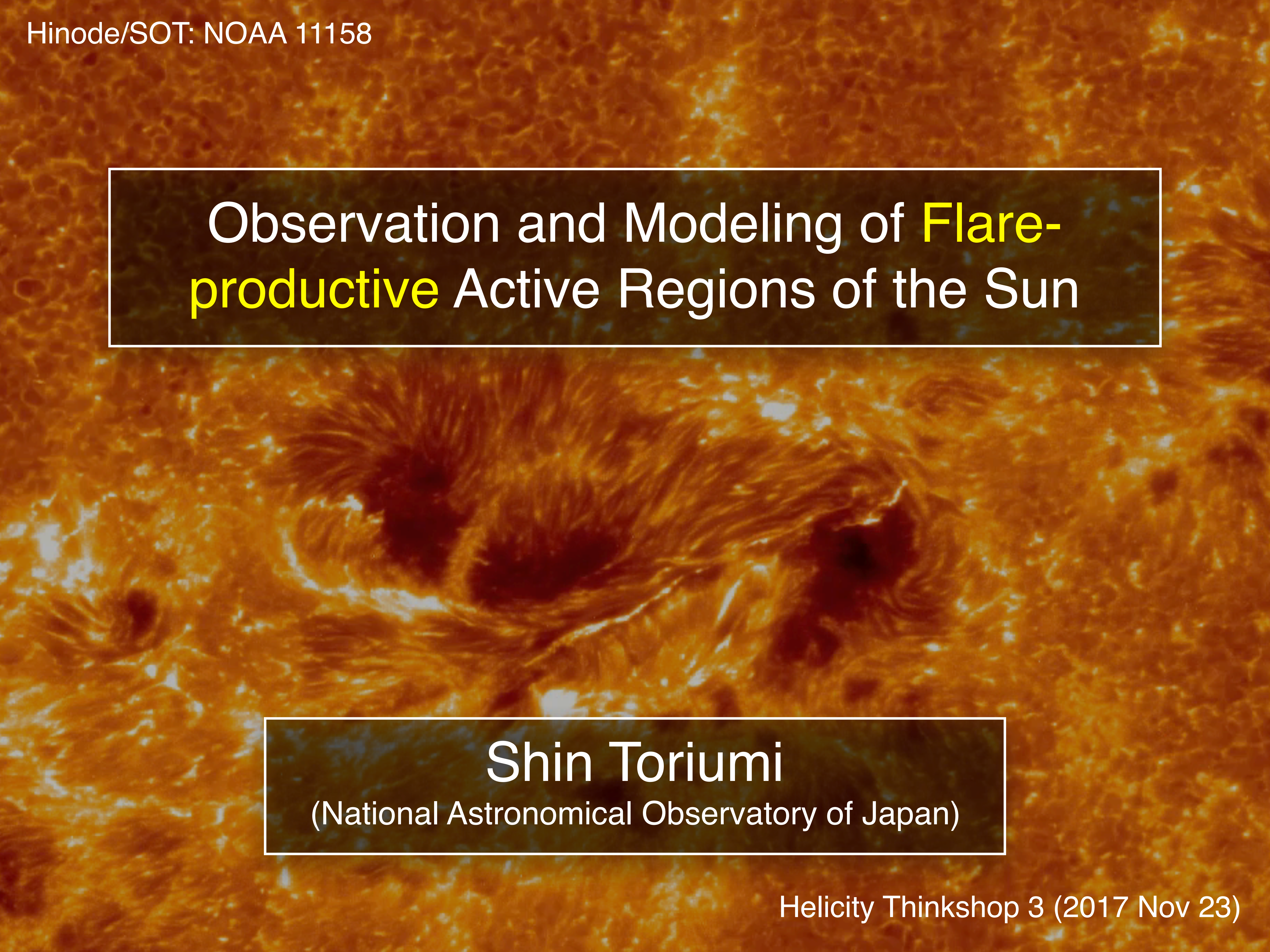
Hinode/SOT: NOAA 11158

Observation and Modeling of Flare-productive Active Regions of the Sun

Shin Toriumi
(National Astronomical Observatory of Japan)

Helicity Thinkshop 3 (2017 Nov 23)

1. Introduction

- Flaring ARs and their formation

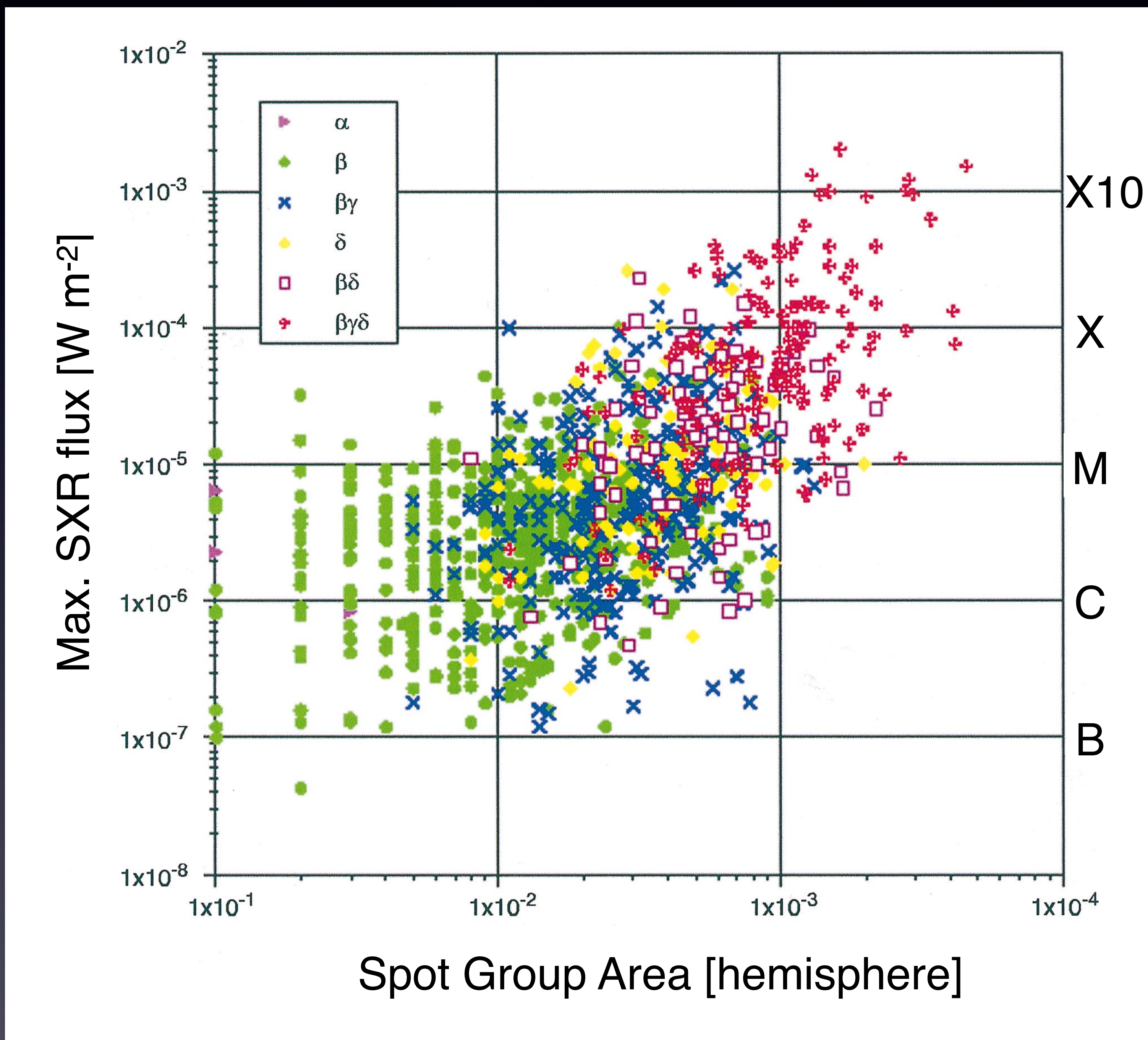

[Sammis+ 2000]

δ-sunspots

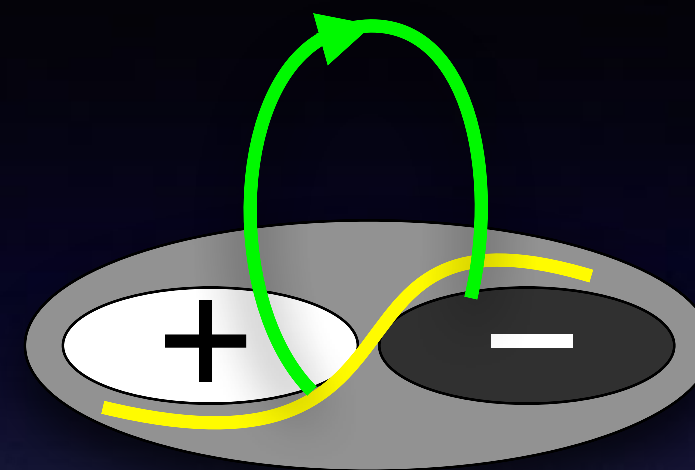

- Sheared PIL
- Sheared arcade

→ high non-potentiality

β-sunspots

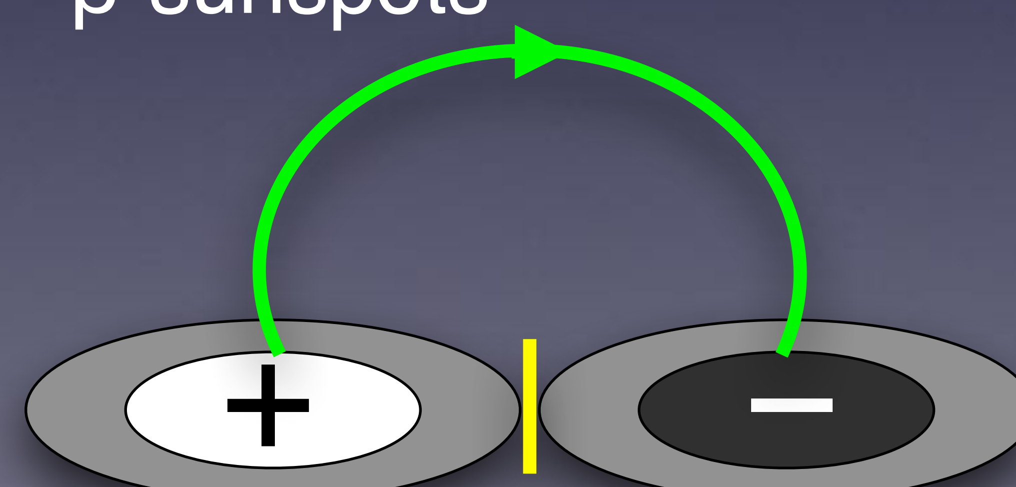

[Künzel 1960]

1. Introduction

- Flaring ARs and their formation
  - δ-sunspots [Künzel 1960, Sammis+ 2000]
  - Sheared PIL [Hagyard+ 1984, Tanaka 1991]
  - Twisted flux tubes [Kurokawa 1987, Leka+ 1996]
  - Complex multipolar spots [Zirin & Tanaka 1973]
  - etc…

↓

Energy and helicity accumulate through magnetic flux emergence*

- This talk: observation and modeling
  - Statistical observation to see the trends of flaring ARs with minimum selection bias
    [Toriumi, Schrijver, Harra, Hudson, & Nagashima 2017 ApJ]
  - Flux-emergene simulaitons to find the cause of observed magnetic structures
    [Toriumi & Takasao 2017 ApJ]

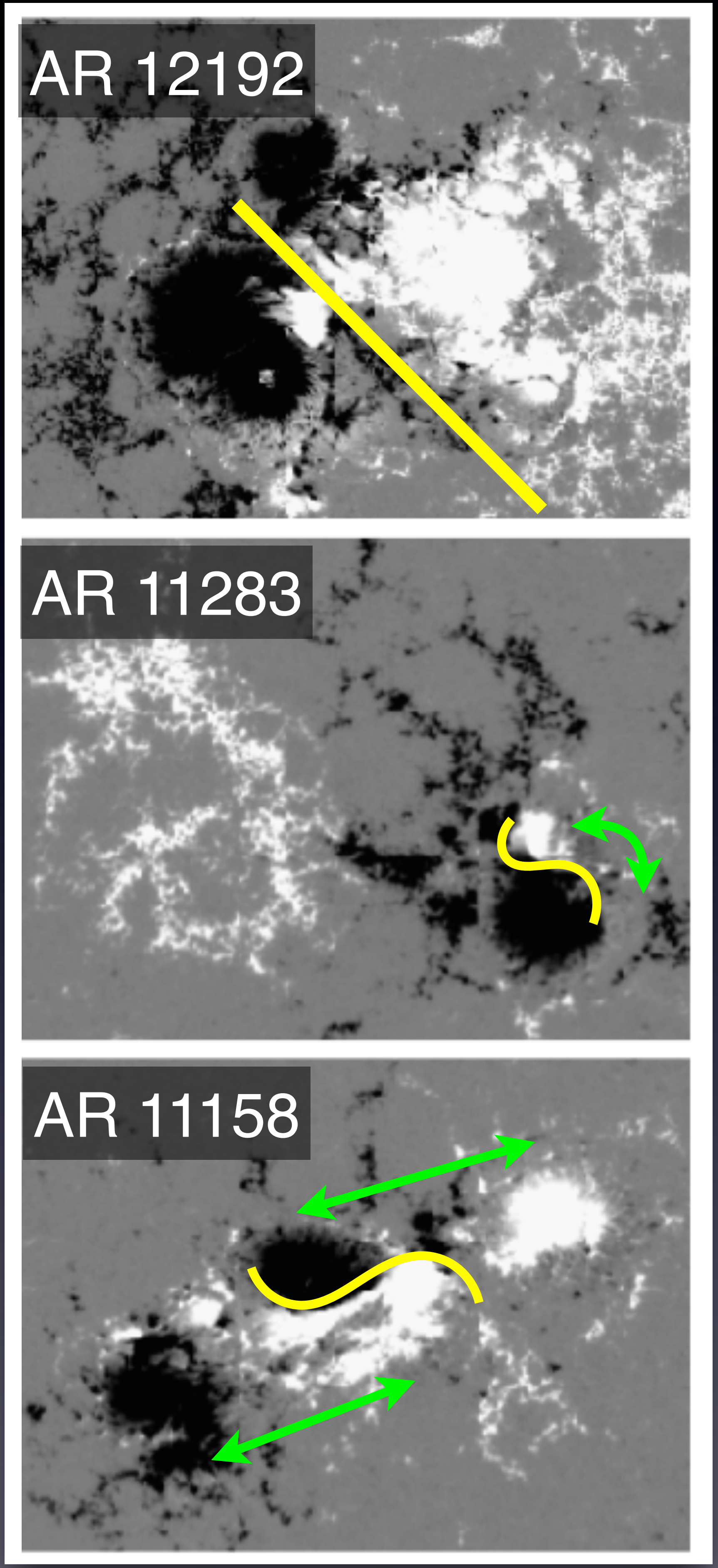

[＊ see many presentations of this week!]

2. Observation

- Flare events
  - Solar Cycle 24: May 2010 — April 2016 (6 years from beginning to declining phase)
  - All ≥M5.0 flares with heliocentric angle $\theta \leq 45$ deg (i.e. $\mu = \cos\theta \geq 0.71$)
  - 51 flares (20 X + 31 M-class) from 29 ARs

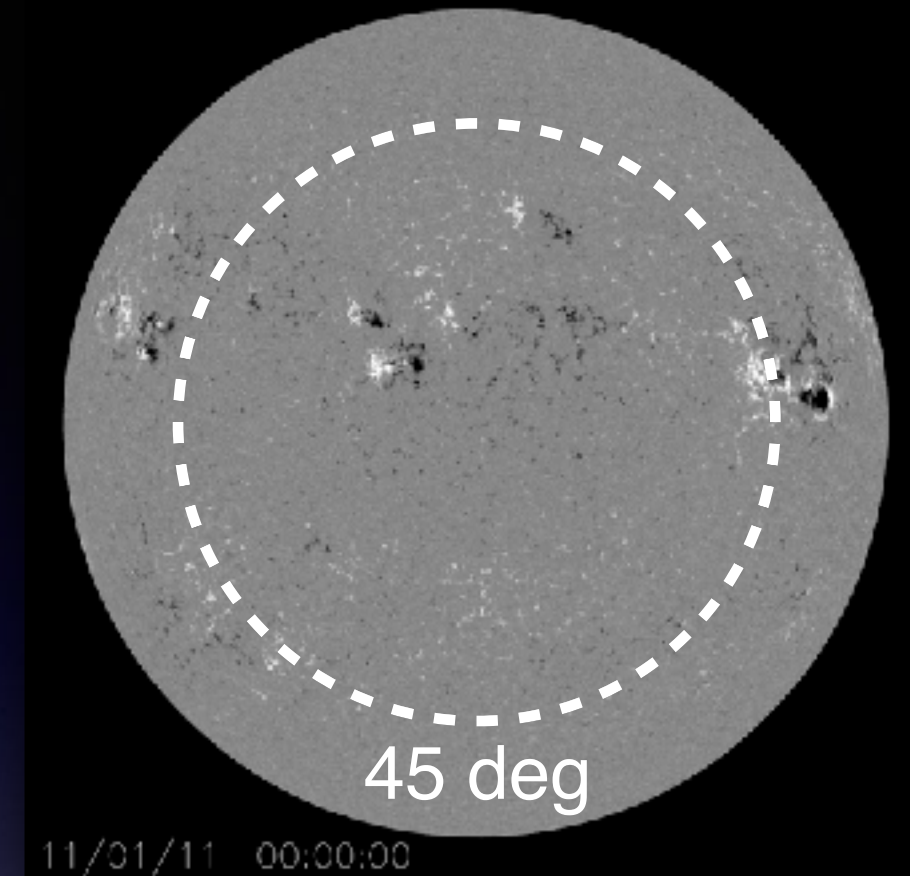

- Data sets
  - Optical/UV: SDO/HMI and AIA mtrack-ed data
  - SXR: GOES light curves
  - CME: SOHO/LASCO CDAW

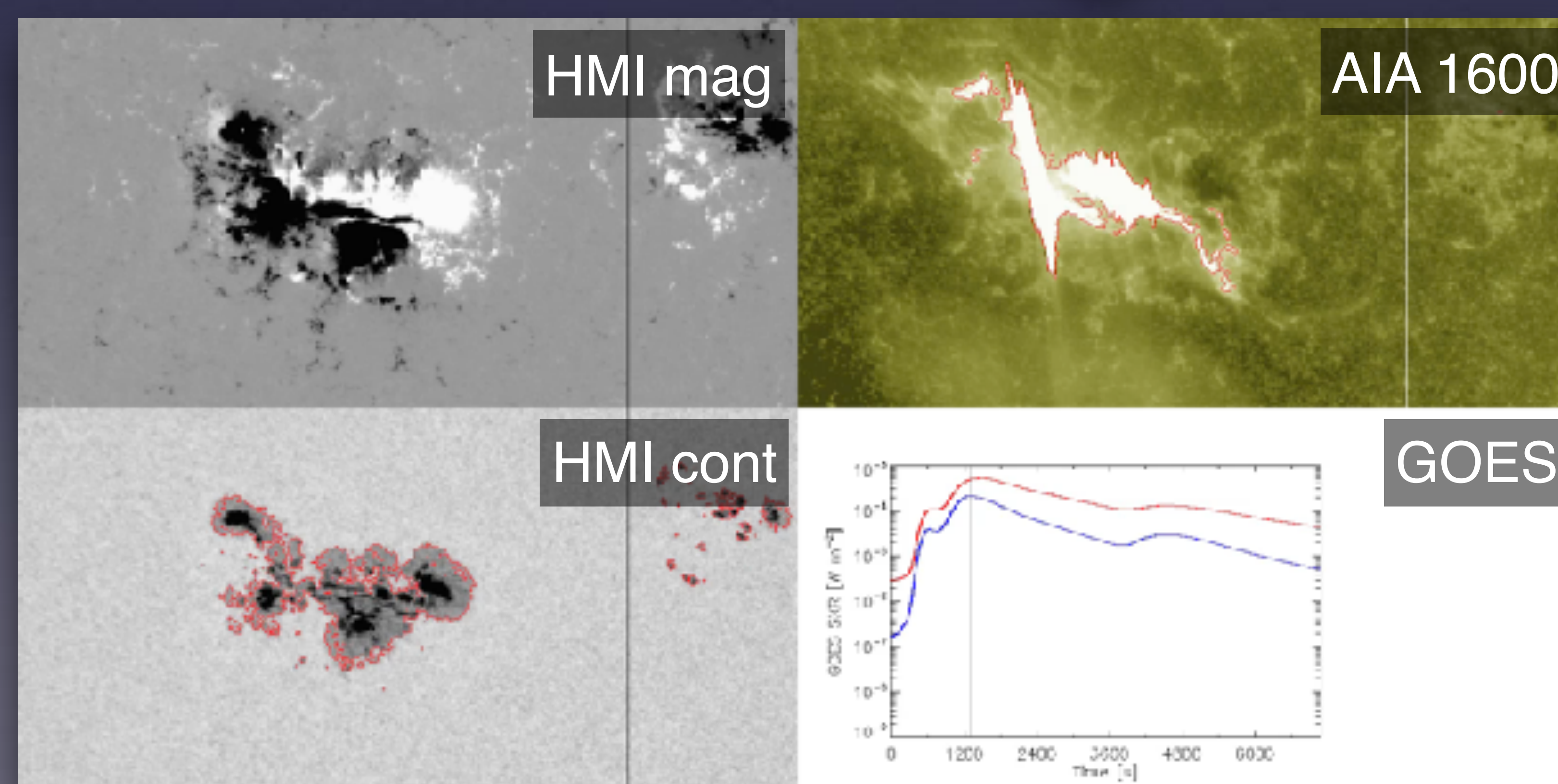

2. Observation

- AR properties

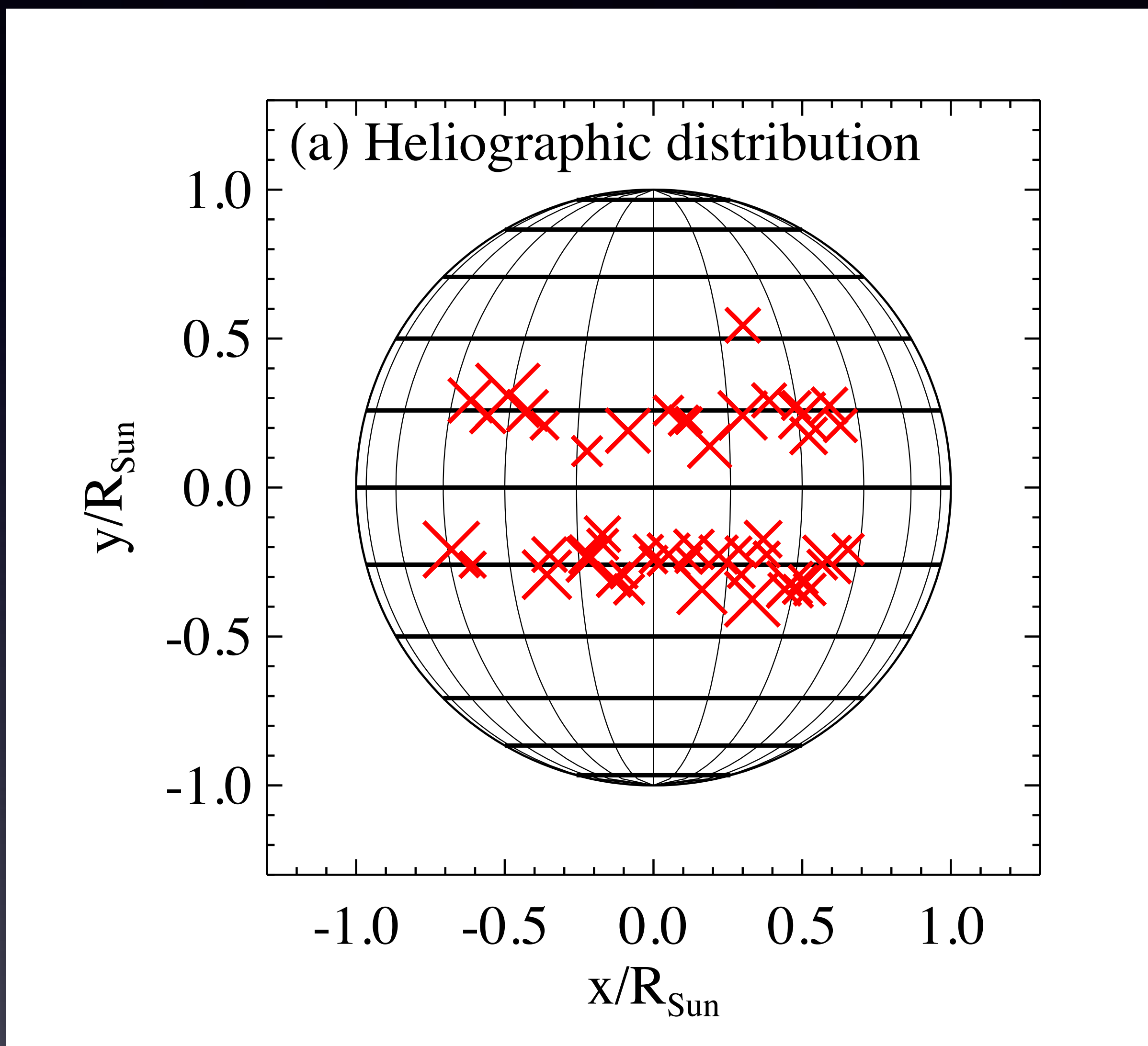

Symbol size varies with the GOES level from M5.0 to X5.4.

- 24 out of 29 ARs (= 83%) show δ-sunspots for at least one flare occurrence [Künzel 1960, Sammis+ 2000].

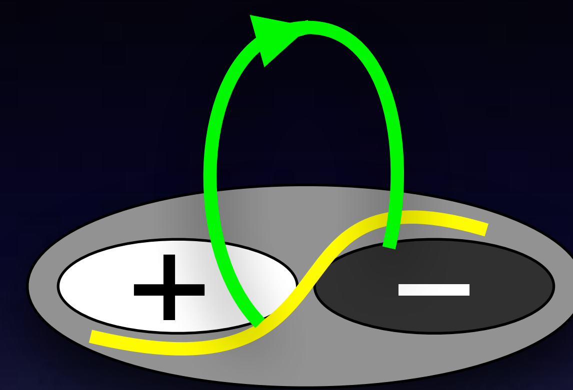

- 4 out of 29 ARs (= 14%) violate Hale's polarity rule for at least one flare occurrence, as opposed to ~4% for all ARs [e.g., Wang & Sheeley 1989, Khlystova & Sokoloff 2009].

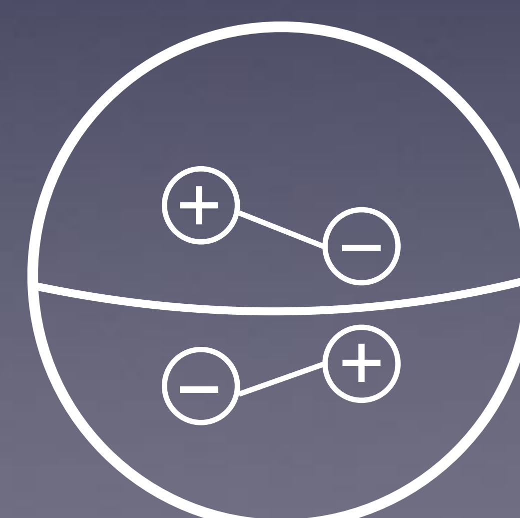

2. Observation

- Categorization of flaring ARs [based on Zirin & Liggett 1987]

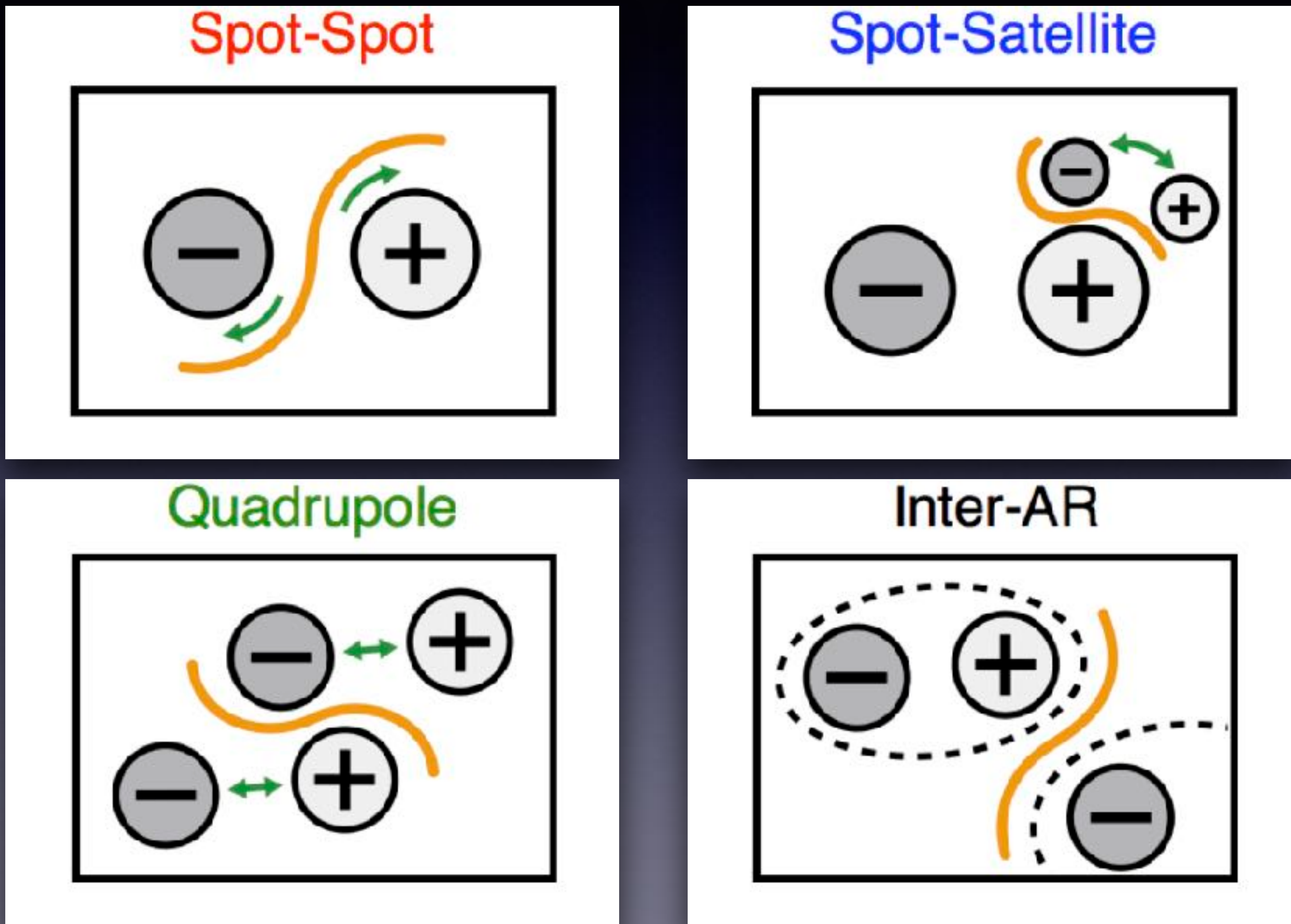

2. Observation

- Categorization of flaring ARs [based on Zirin & Liggett 1987]

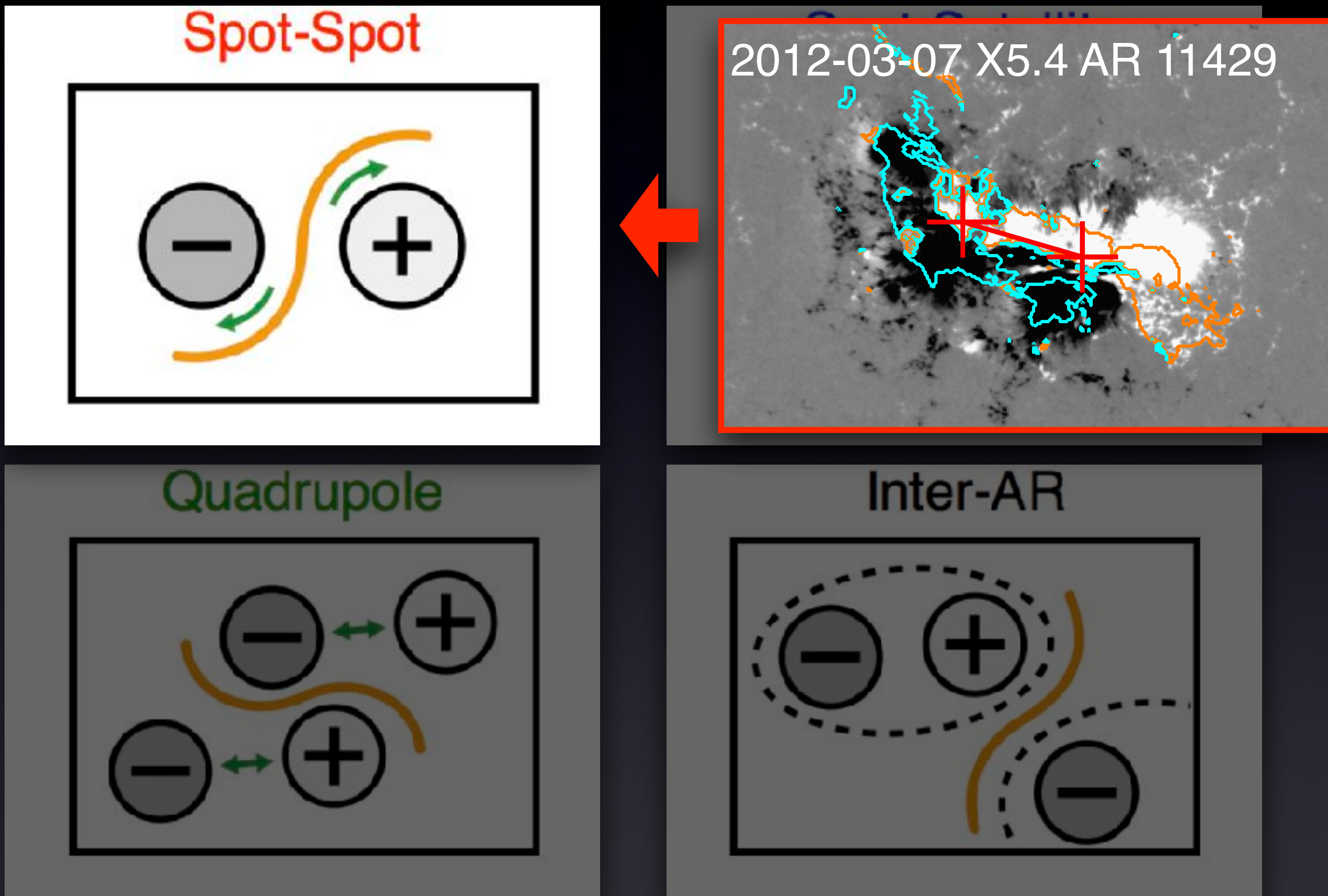

2. Observation

- Categorization of flaring ARs [based on Zirin & Liggett 1987]

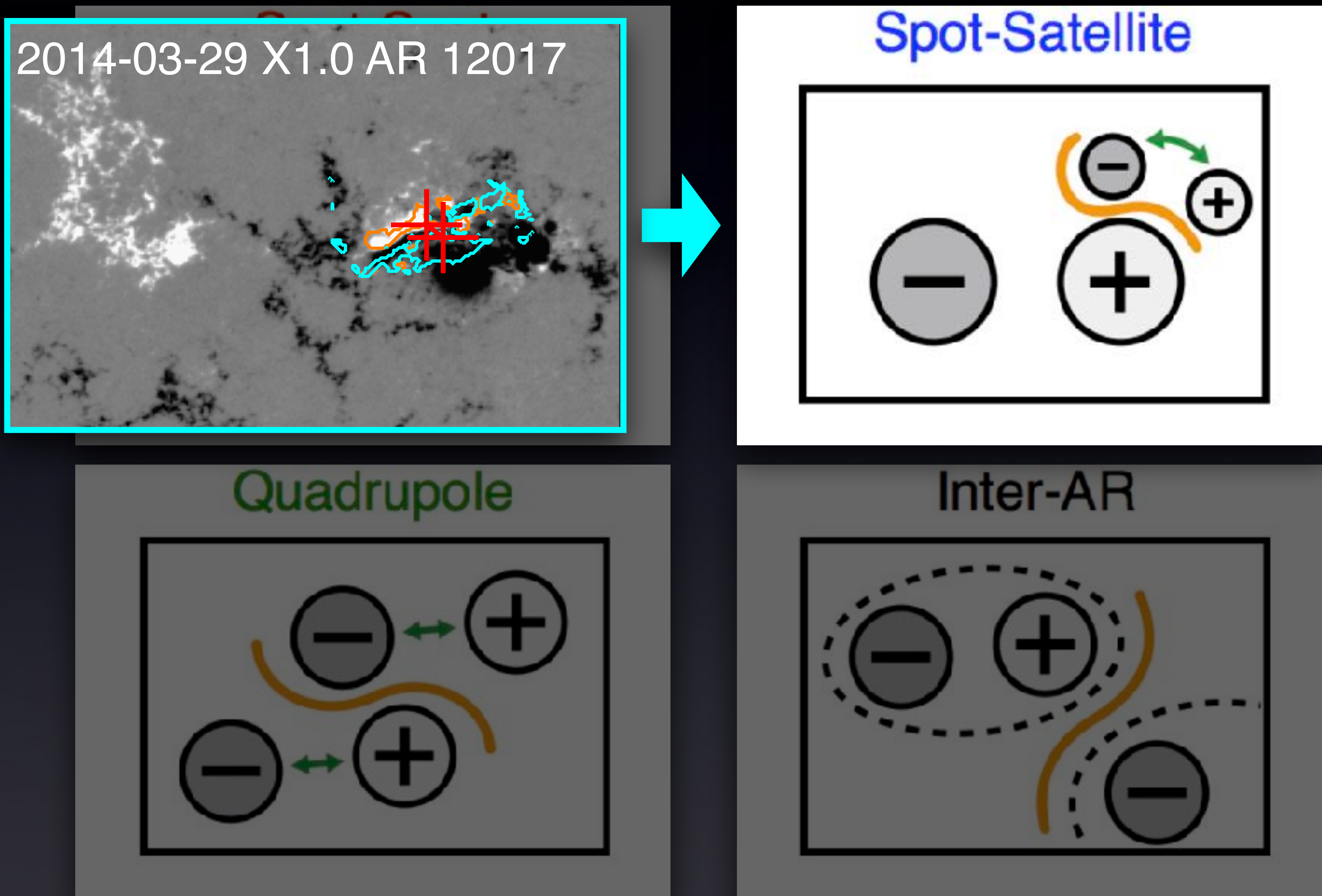

2. Observation

- Categorization of flaring ARs [based on Zirin & Liggett 1987]

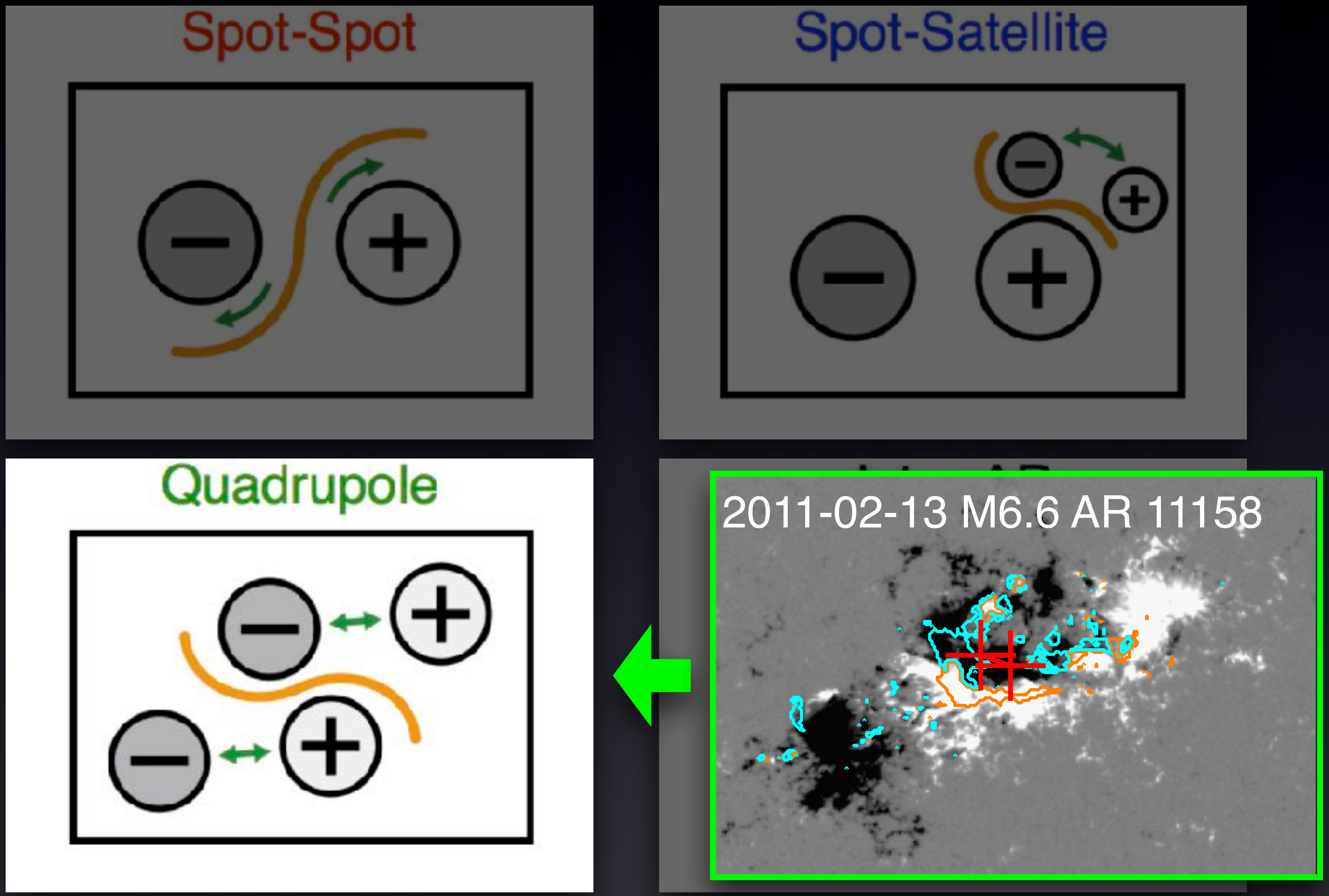

2. Observation

- Categorization of flaring ARs [based on Zirin & Liggett 1987]

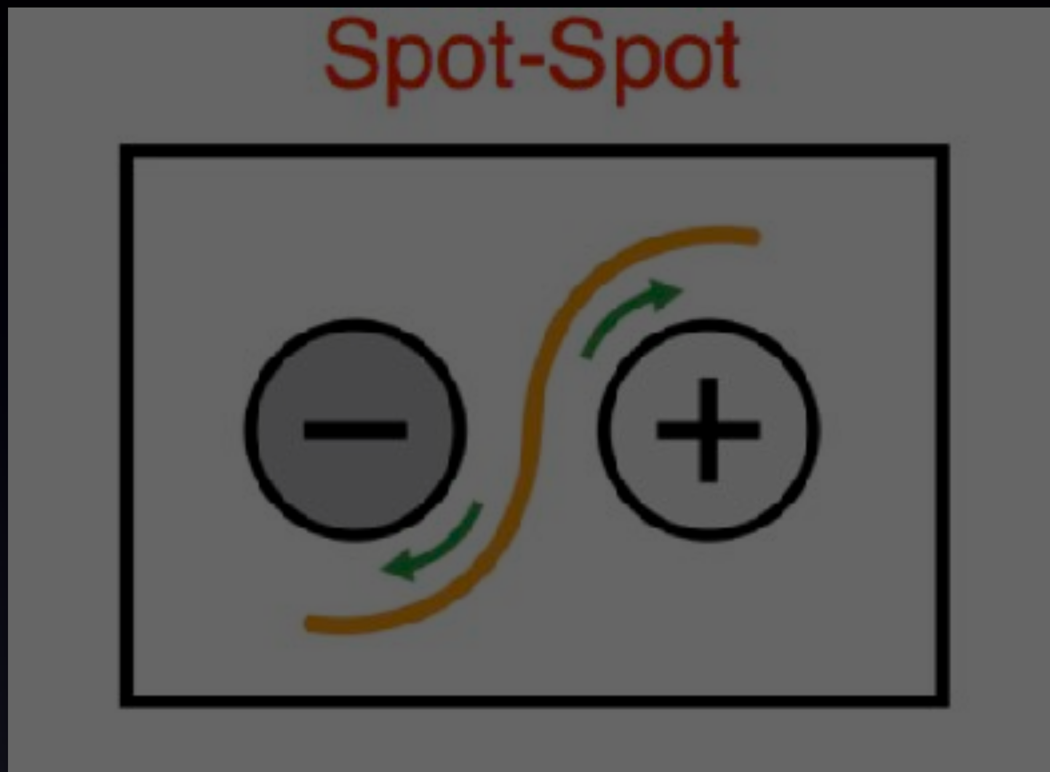

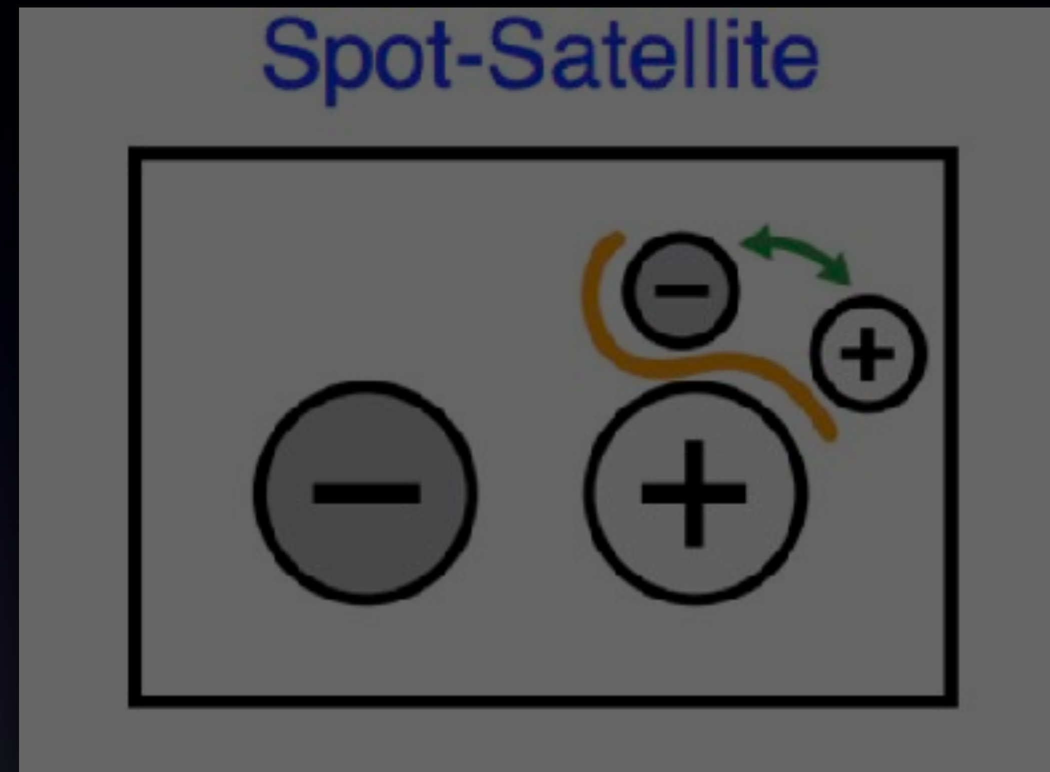

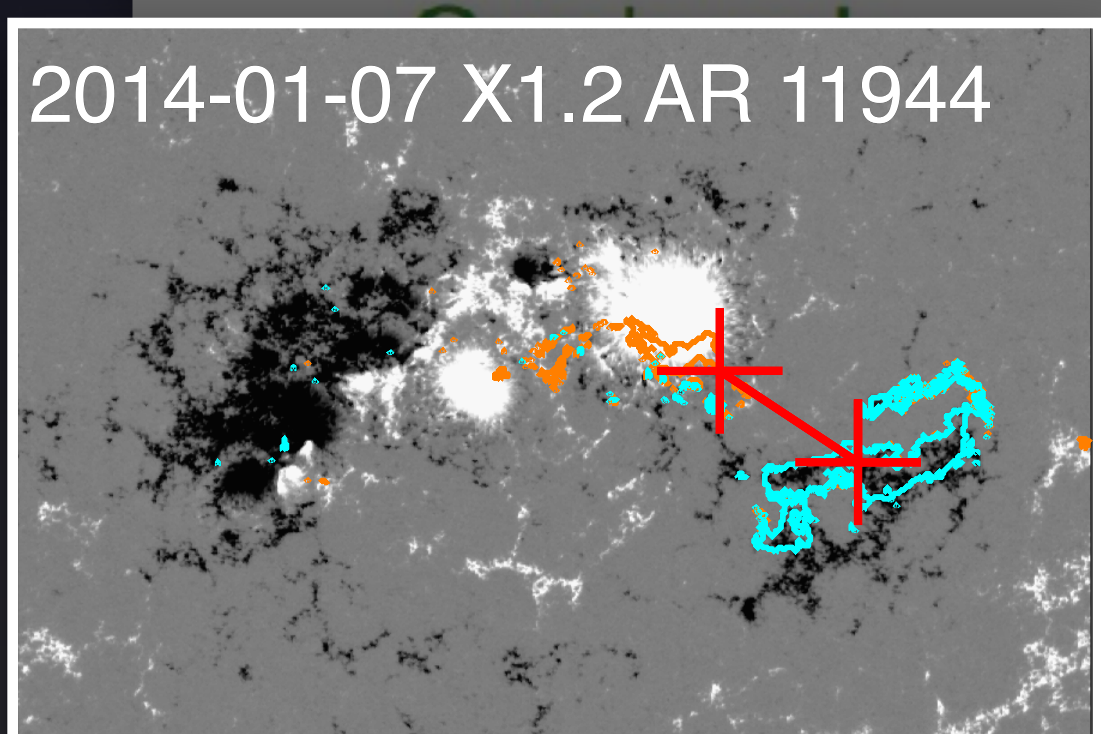

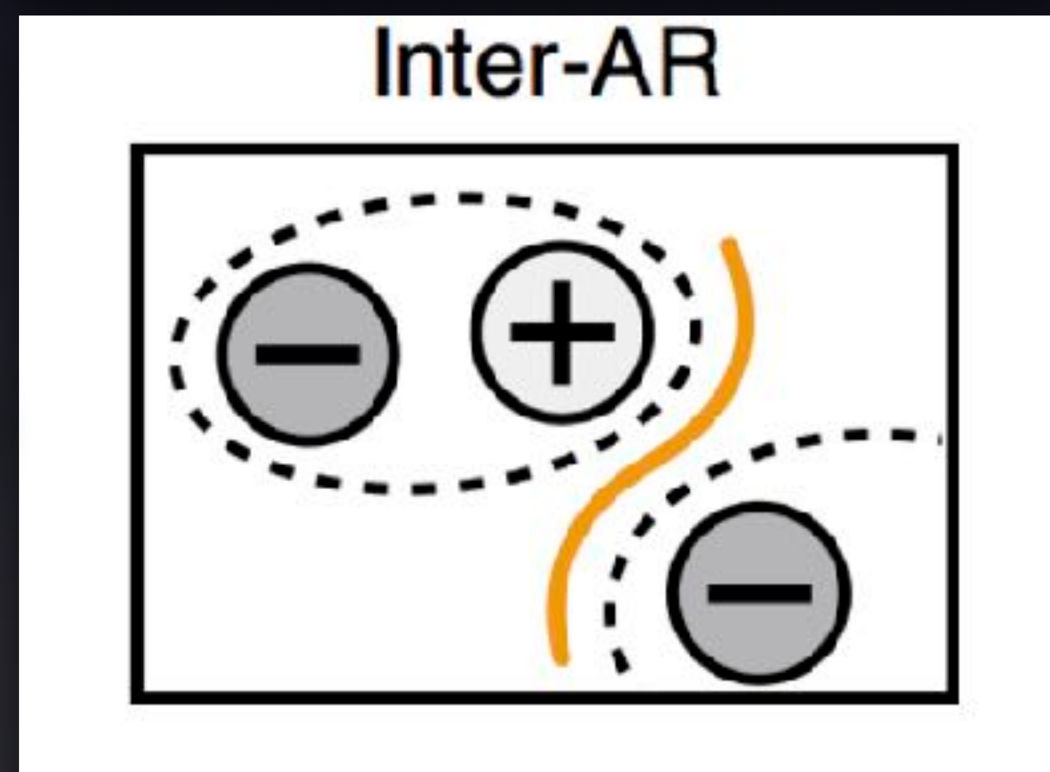

2. Observation

- Categorization of flaring ARs

Fraction

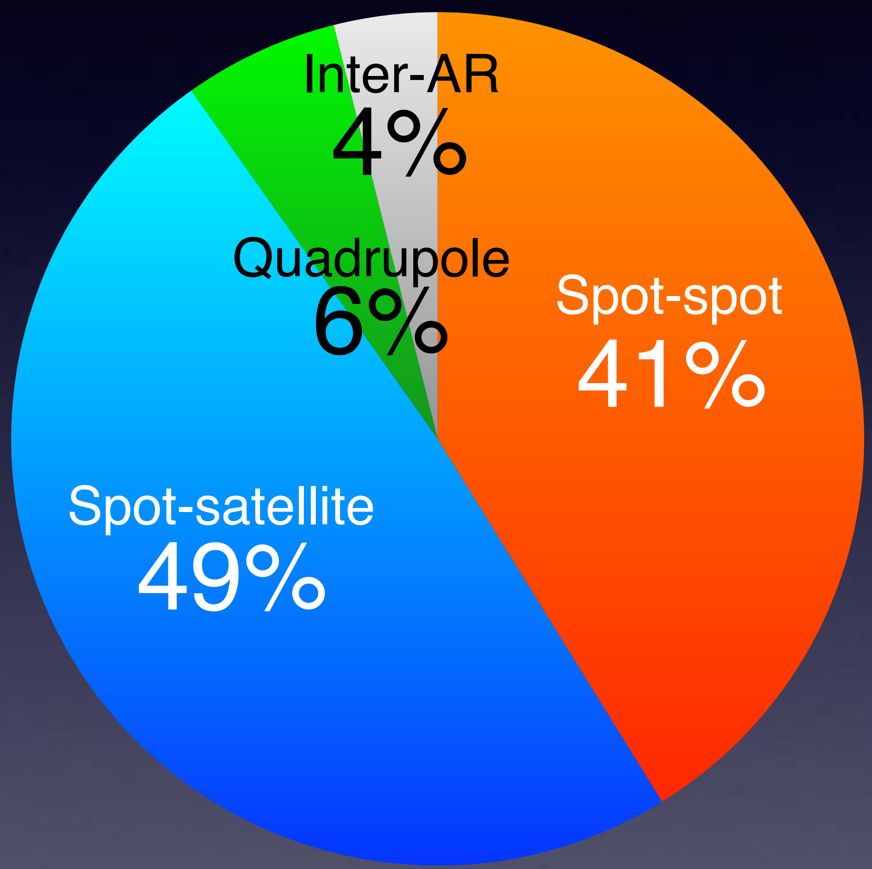

CME productivity

Spot-spot 57% < Spot-satellite 64%

Spot-satellite is slightly more eruptive.
→ Mag structure affects the CME production?

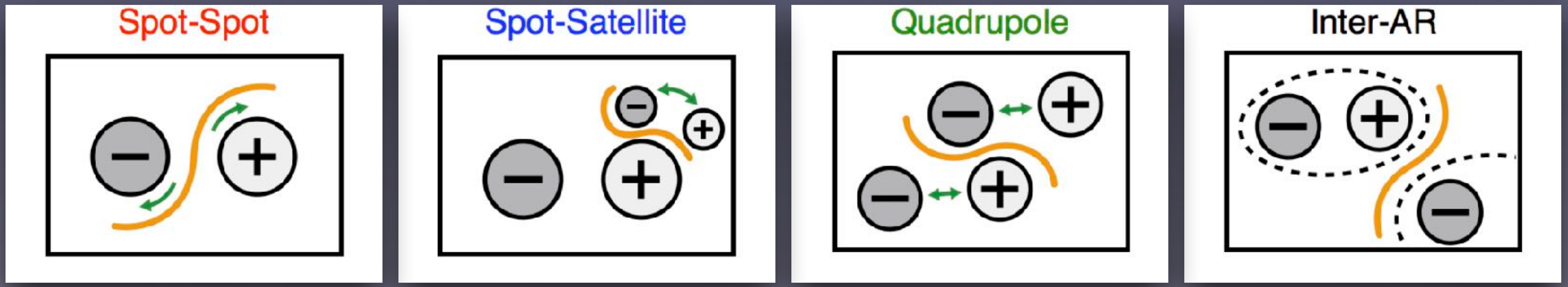

2. Observation

- Categorization of flaring ARs

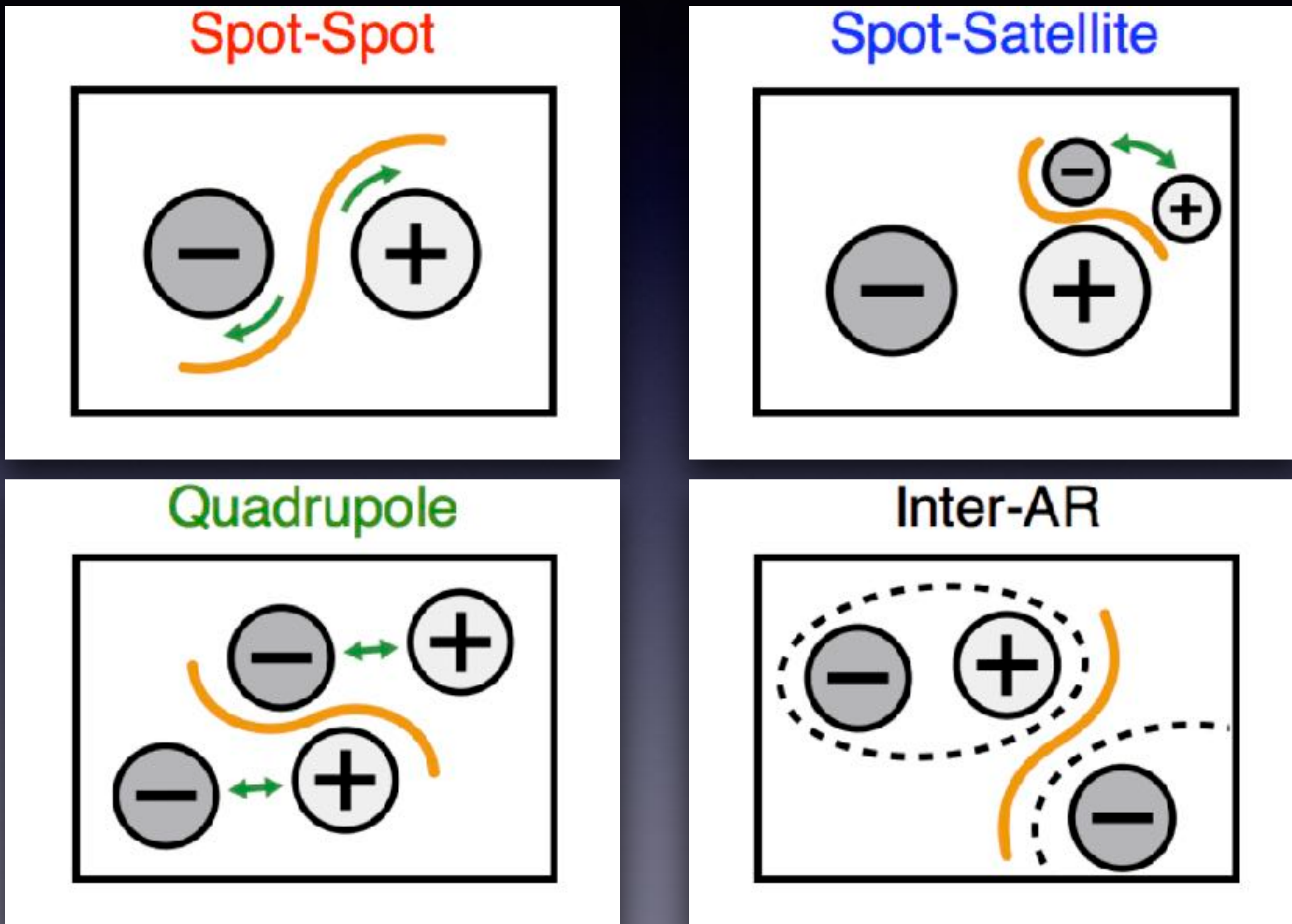

2. Observation

- Categorization of flaring ARs

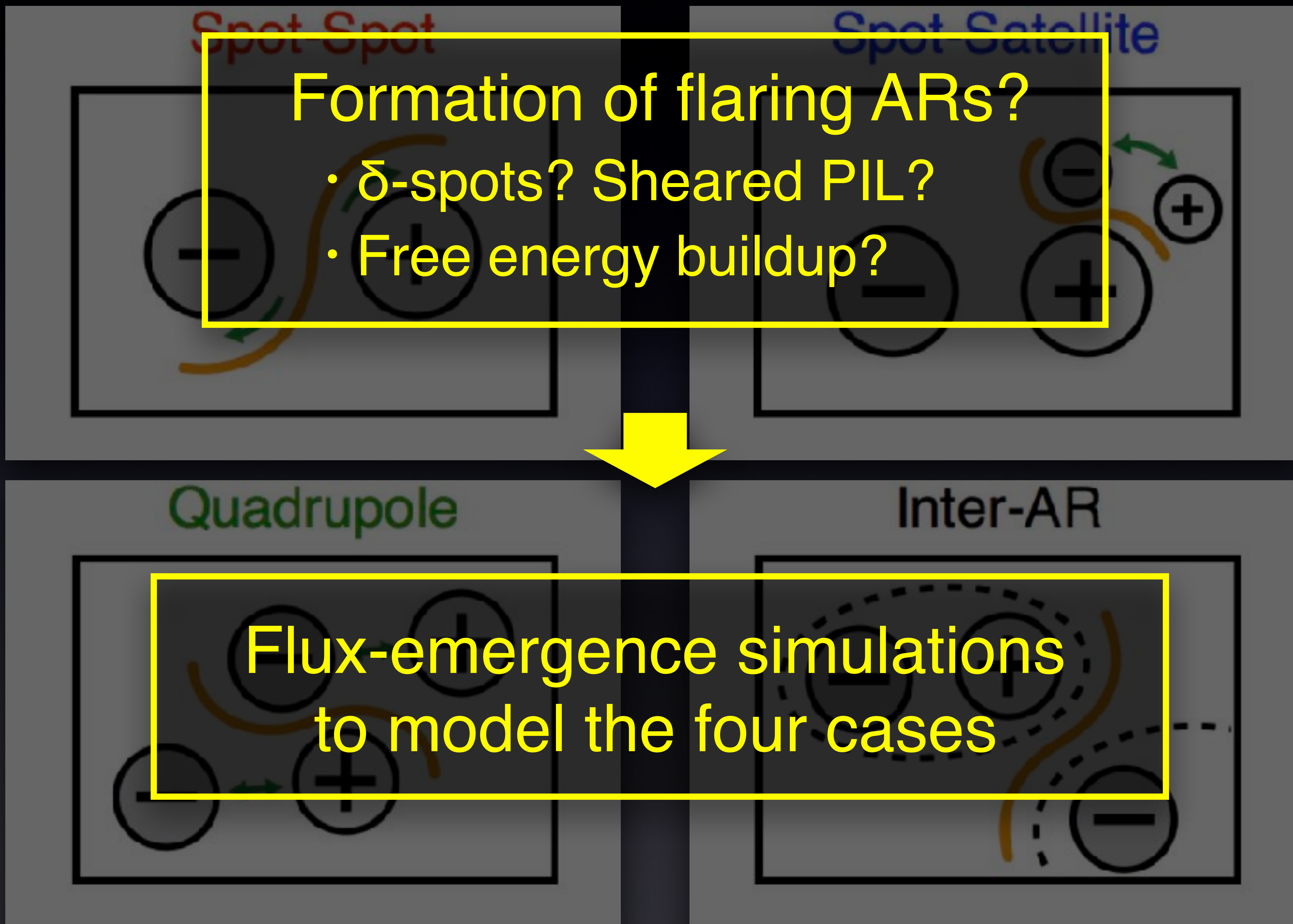

Formation of flaring ARs?

- δ-spots? Sheared PIL?
- Free energy buildup?

Flux-emergence simulations to model the four cases

3. Modeling

- 3D Flux-emergence Simulations (code by Takasao+ 2015)

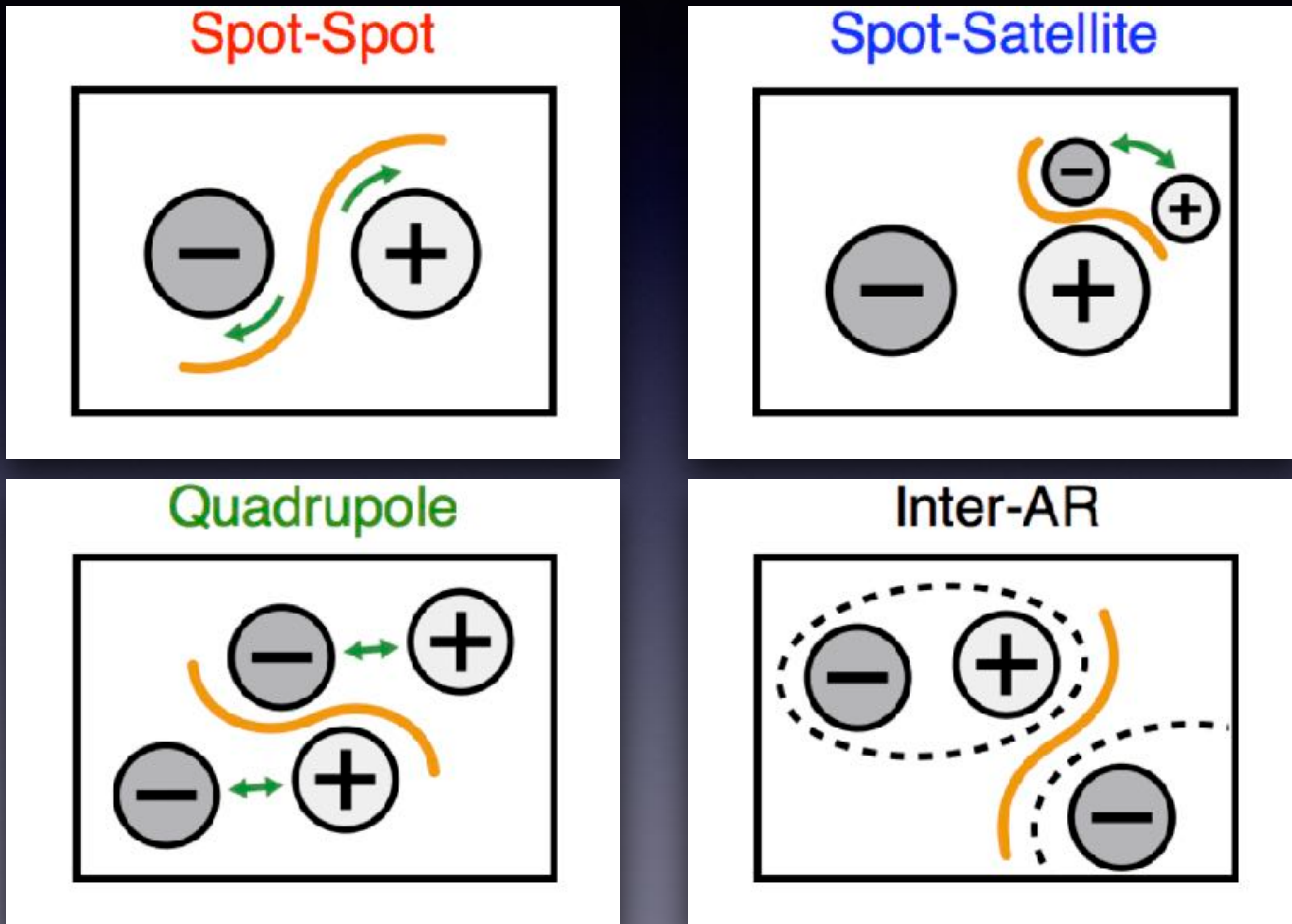

3. Modeling

- 3D Flux-emergence Simulations (code by Takasao+ 2015)

Spot-Spot

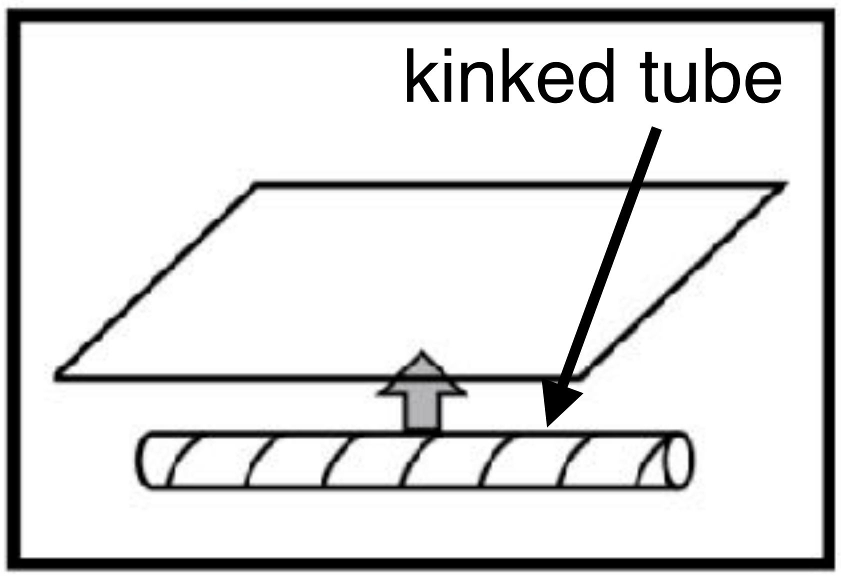

[Linton+ 1996, Fan+ 1999, Takasao+ 2015]

Spot-Satellite

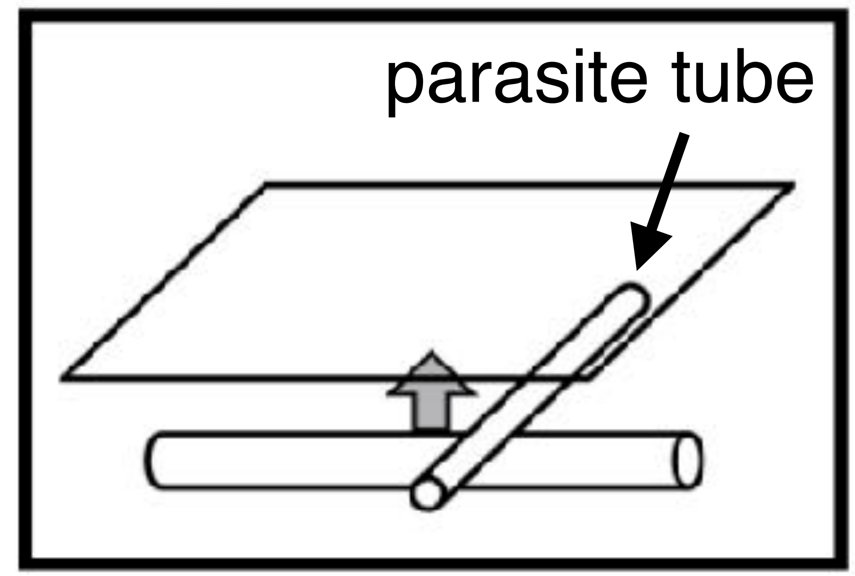

[Linton+ 2005, Cheung+ in prep]

Quadrupole

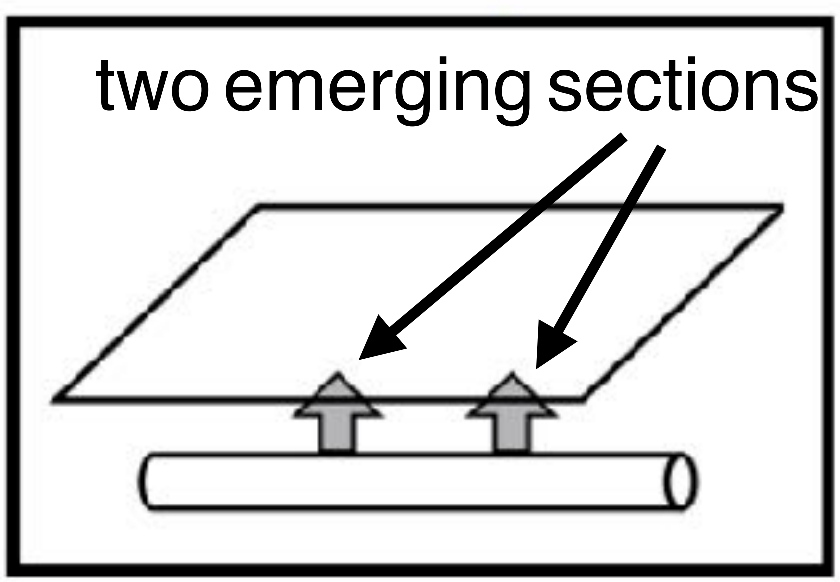

[ST+ 2014, Fang & Fan 2015]

Inter-AR

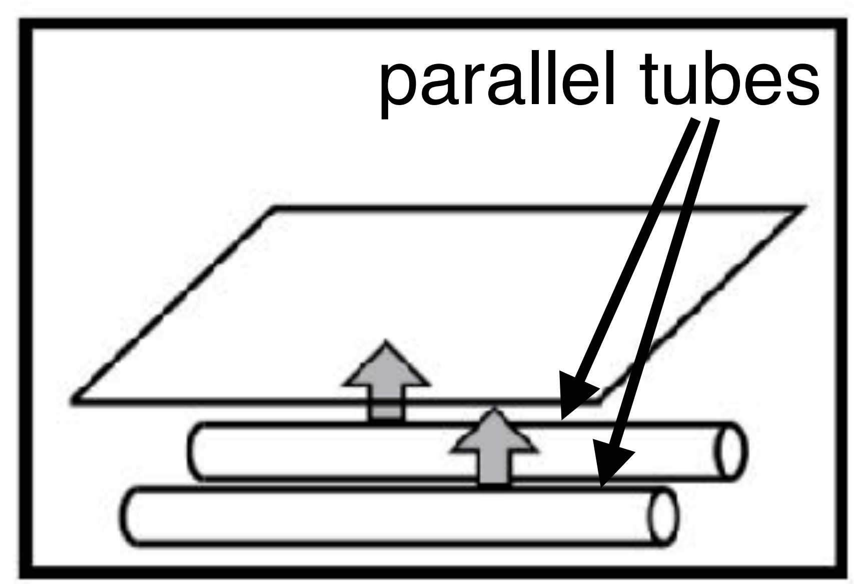

[Fan+ 1998, ST+ 2014]

3. Modeling

- Magnetogram + Field Lines → δ-spots with Sheared PIL

Spot-Spot

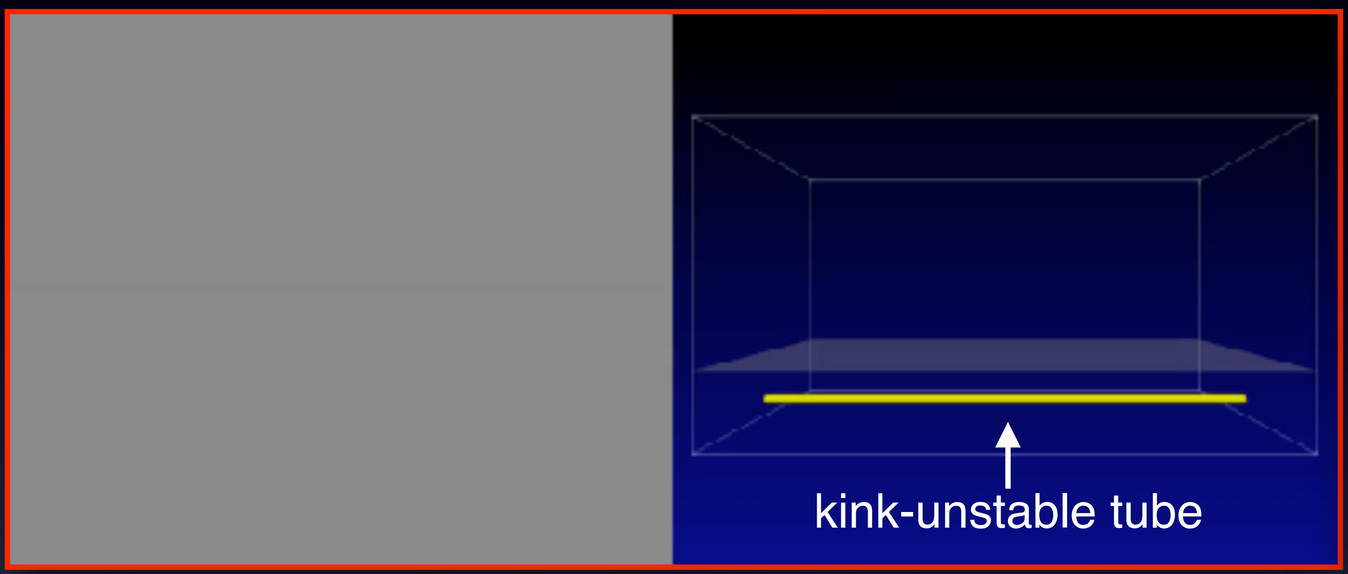

Spot-Satellite

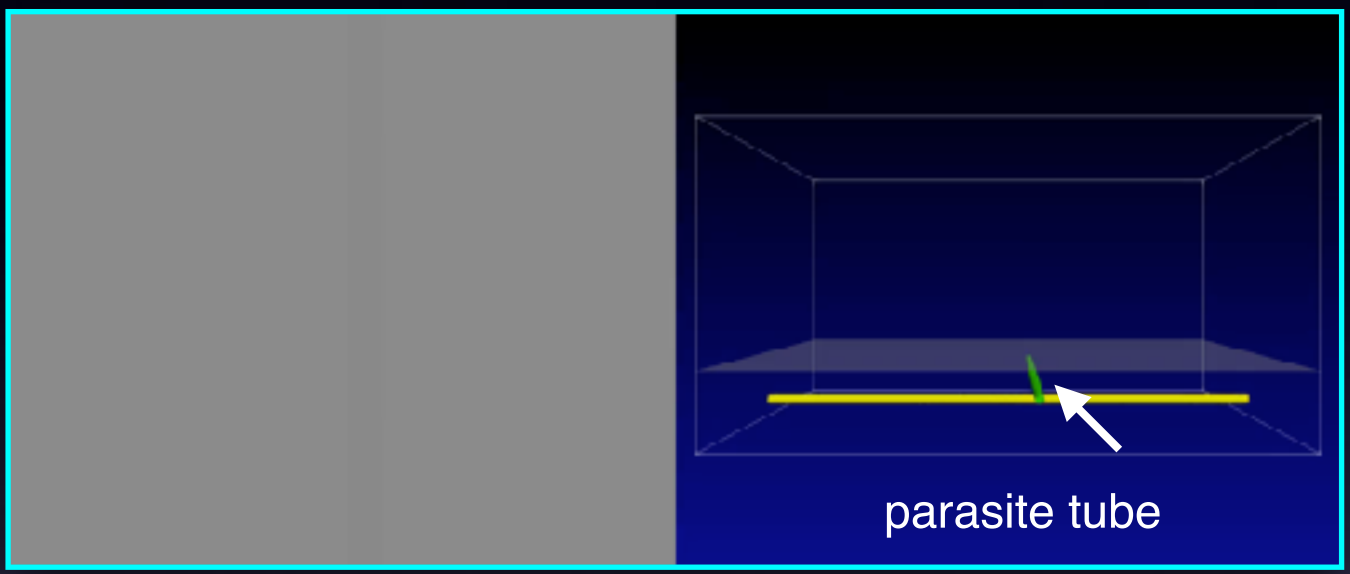

Quadrupole

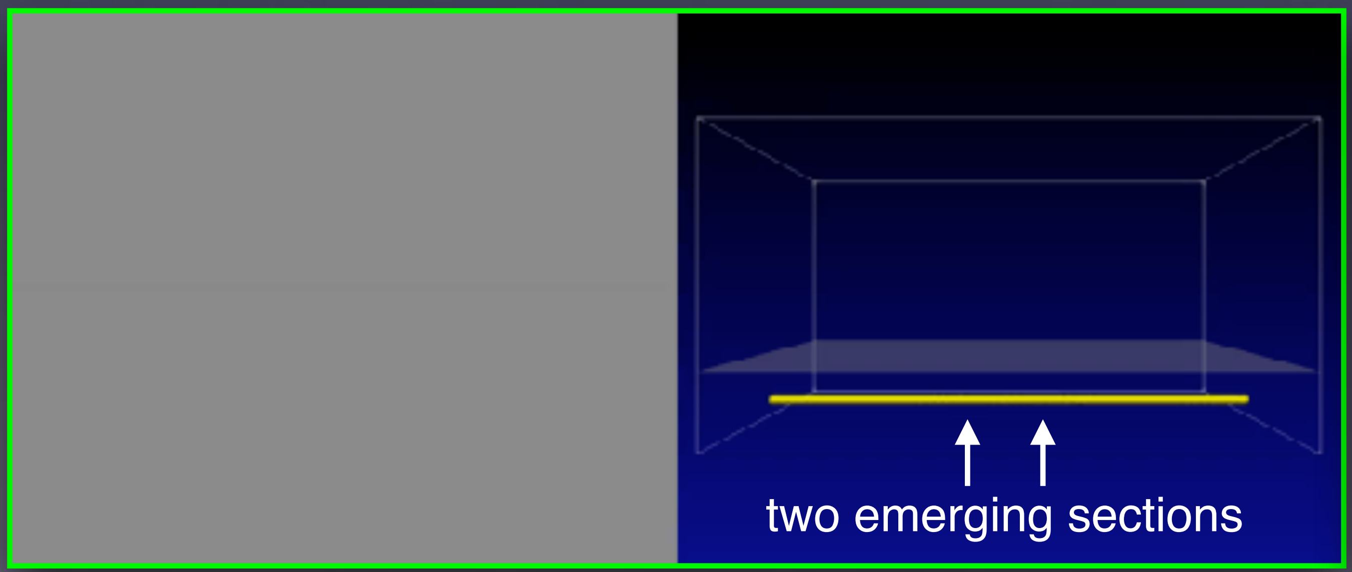

Inter-AR

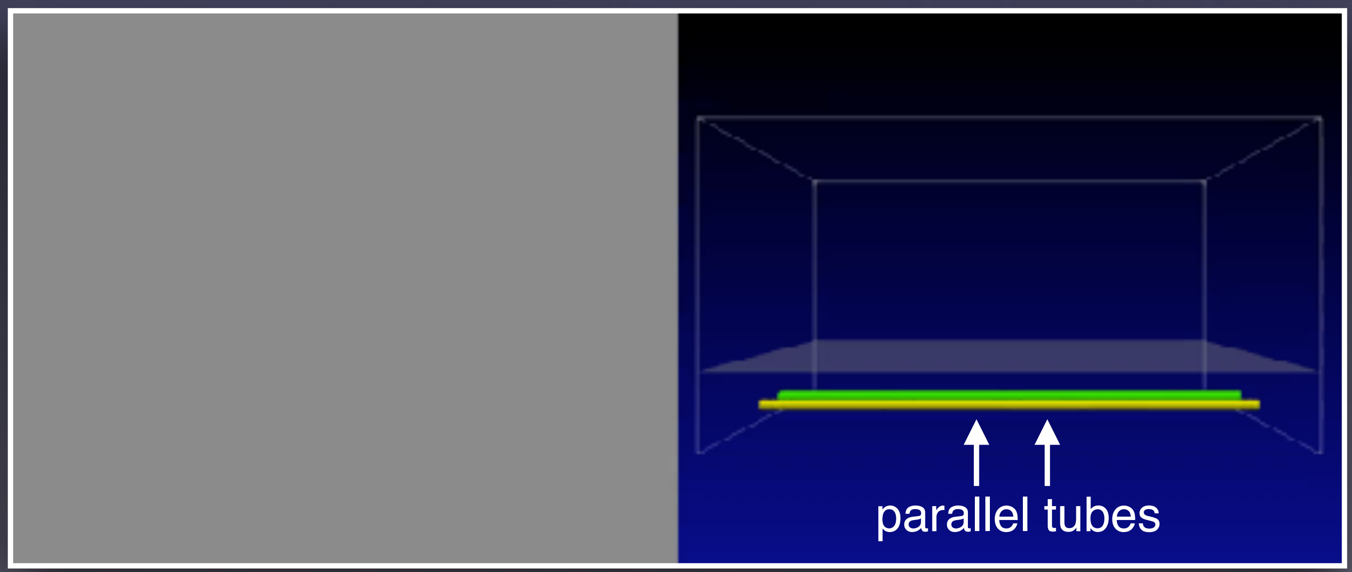

3. Modeling

- Magnetogram + Field Lines → δ-spots with Sheared PIL

Spot-Spot

Spot-Satellite

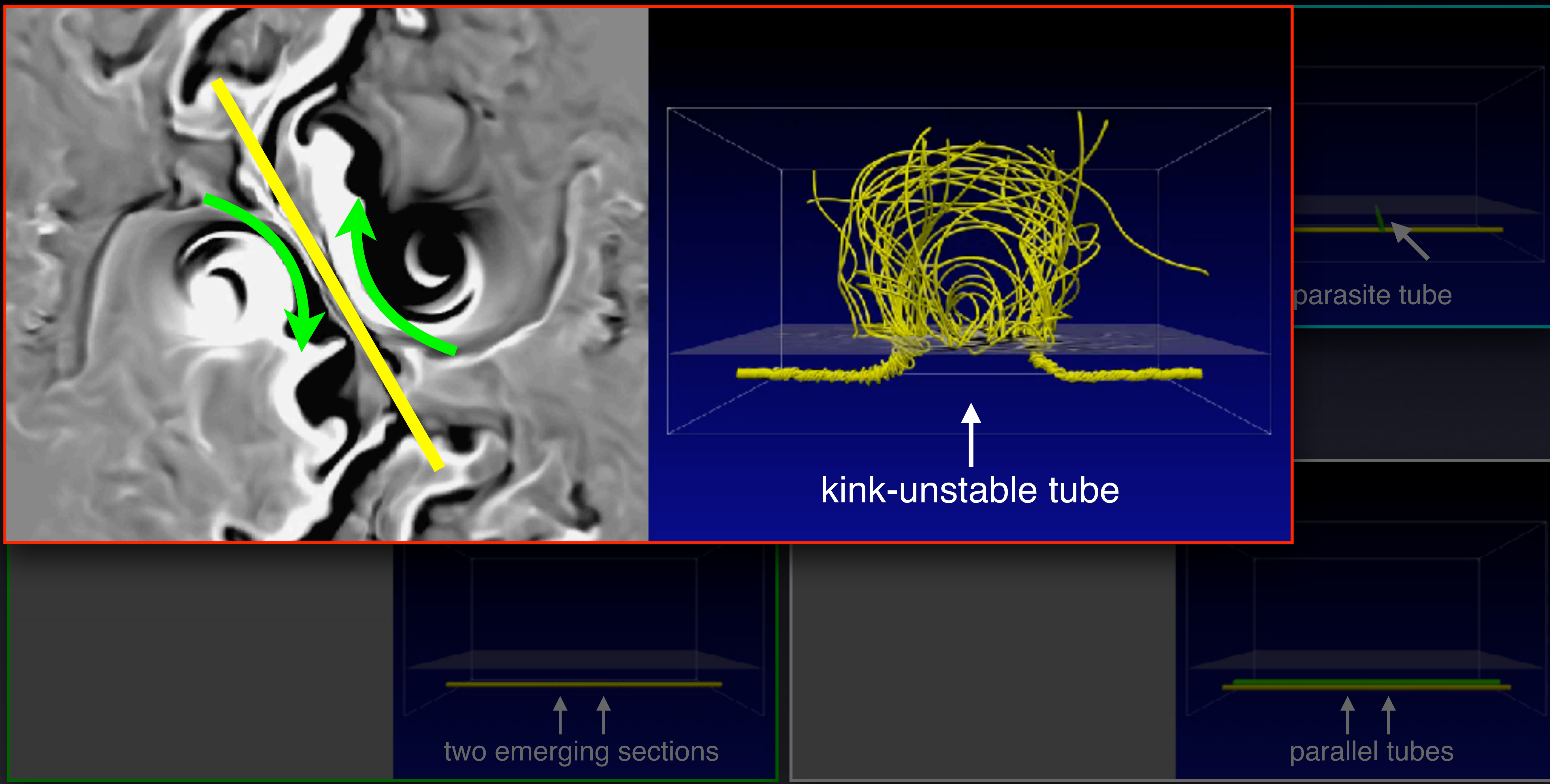

3. Modeling

- Magnetogram + Field Lines → δ-spots with Sheared PIL

Spot-Spot

Spot-Satellite

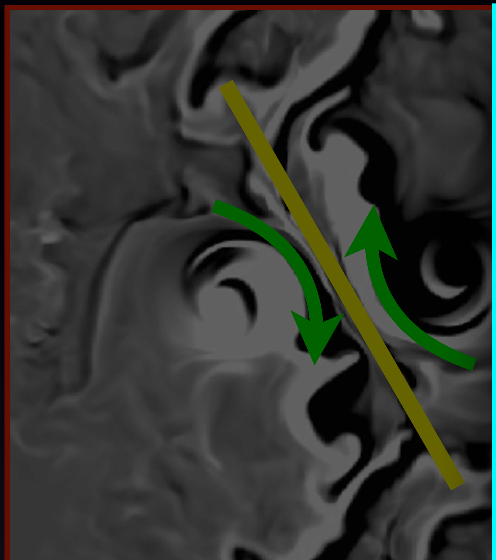

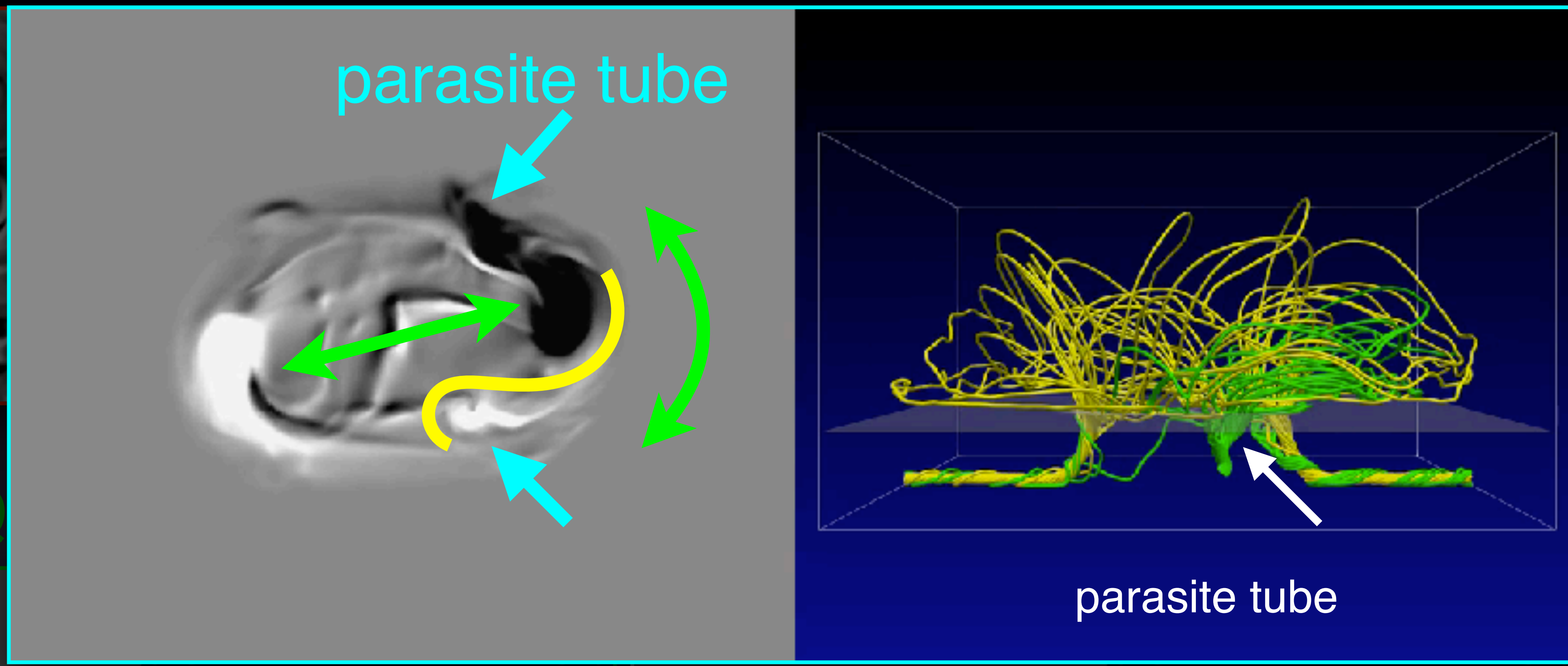

Q

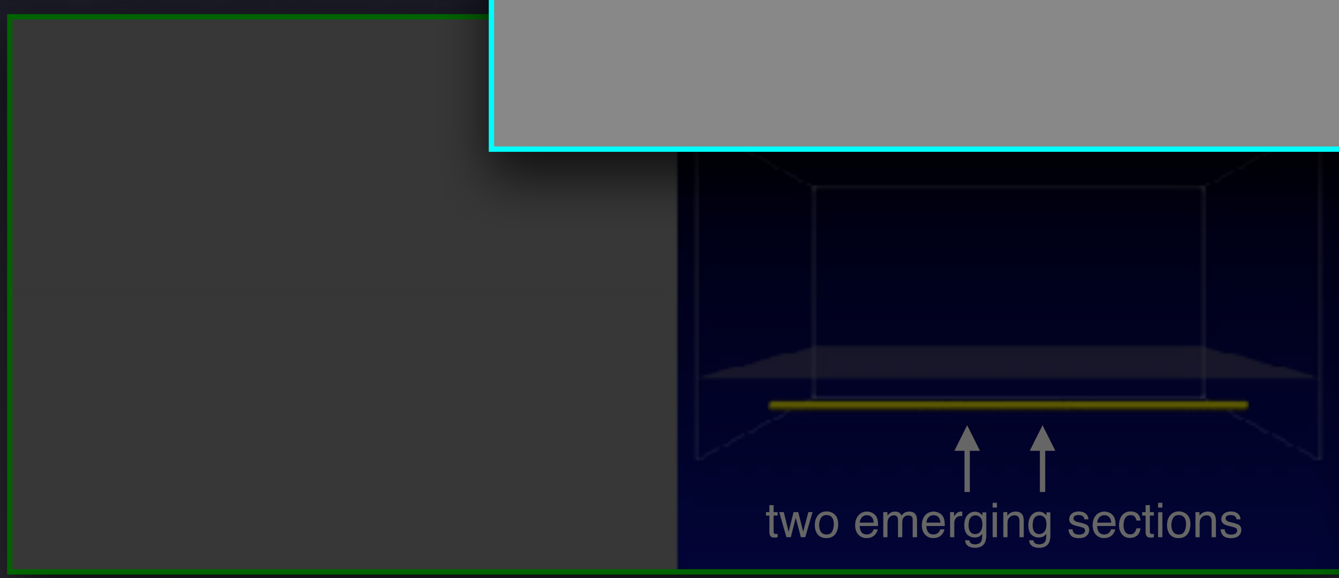

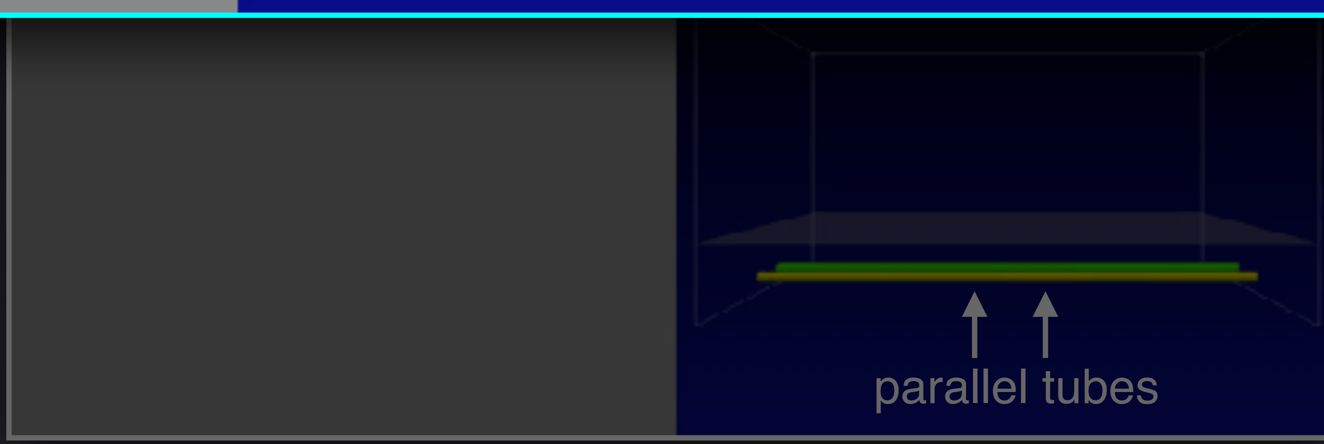

3. Modeling

- Magnetogram + Field Lines → δ-spots with Sheared PIL

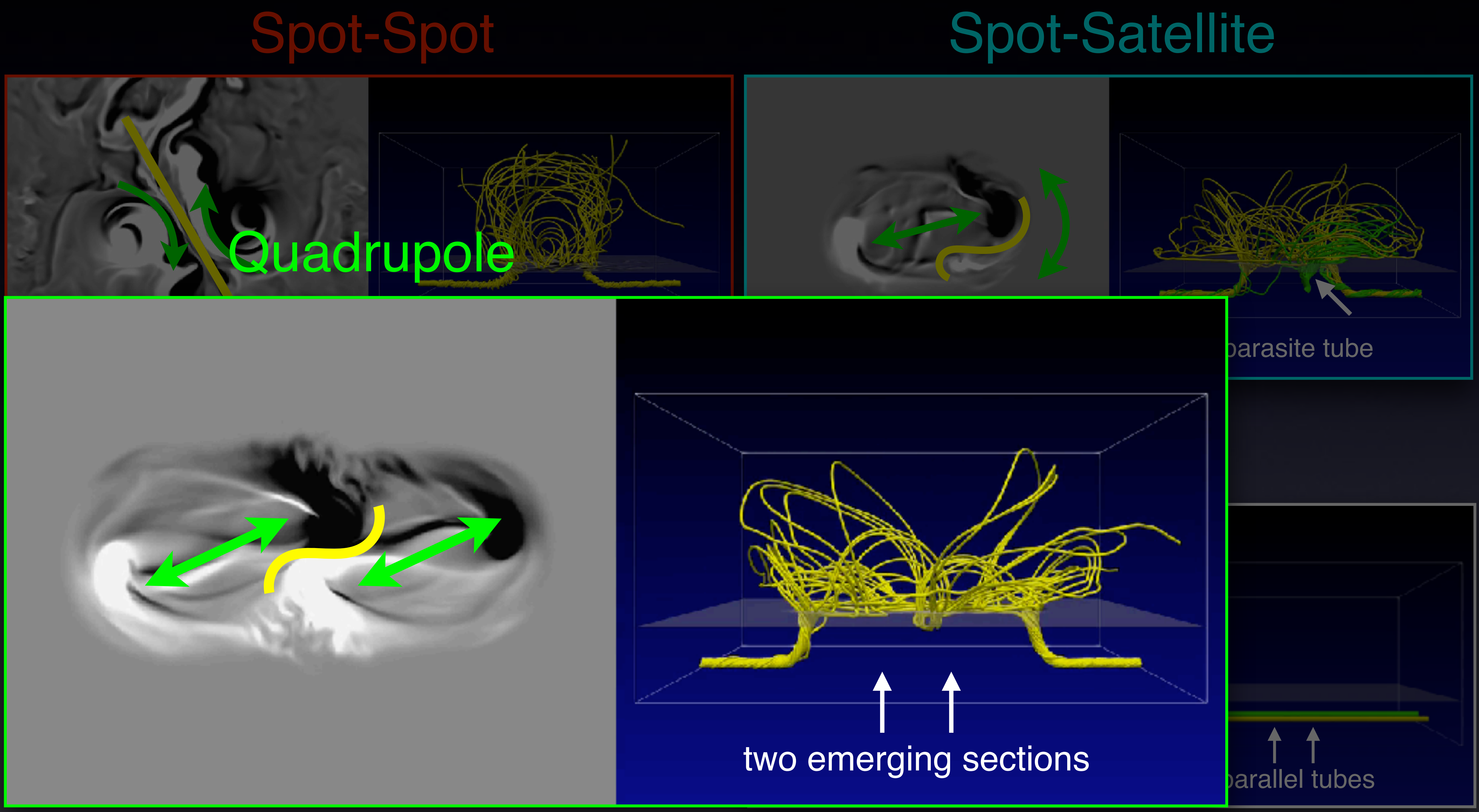

3. Modeling

- Magnetogram + Field Lines → δ-spots with Sheared PIL

Spot-Spot

Spot-Satellite

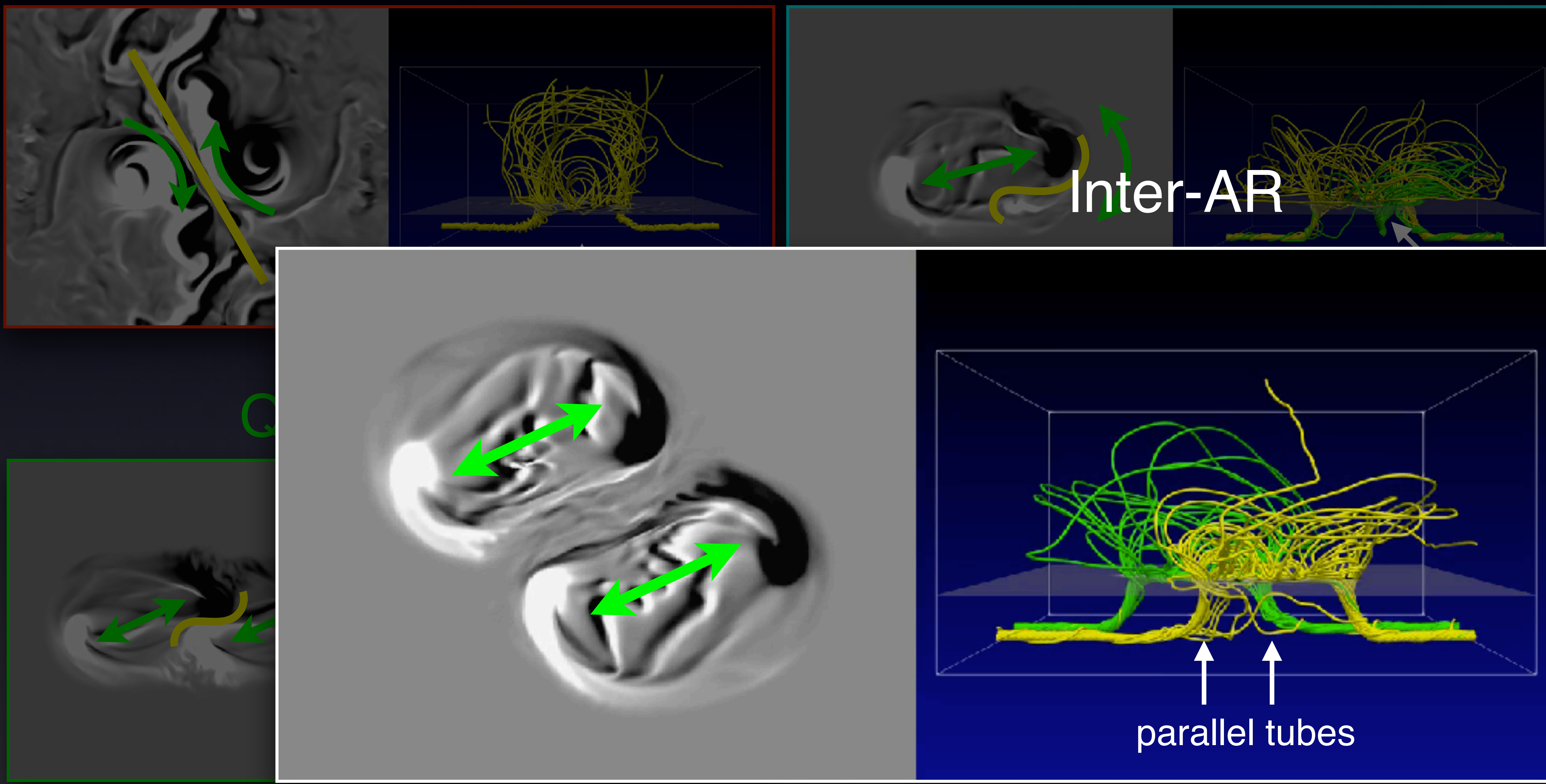

3. Modeling

- Magnetogram + Field Lines → δ-spots with Sheared PIL

Spot-Spot

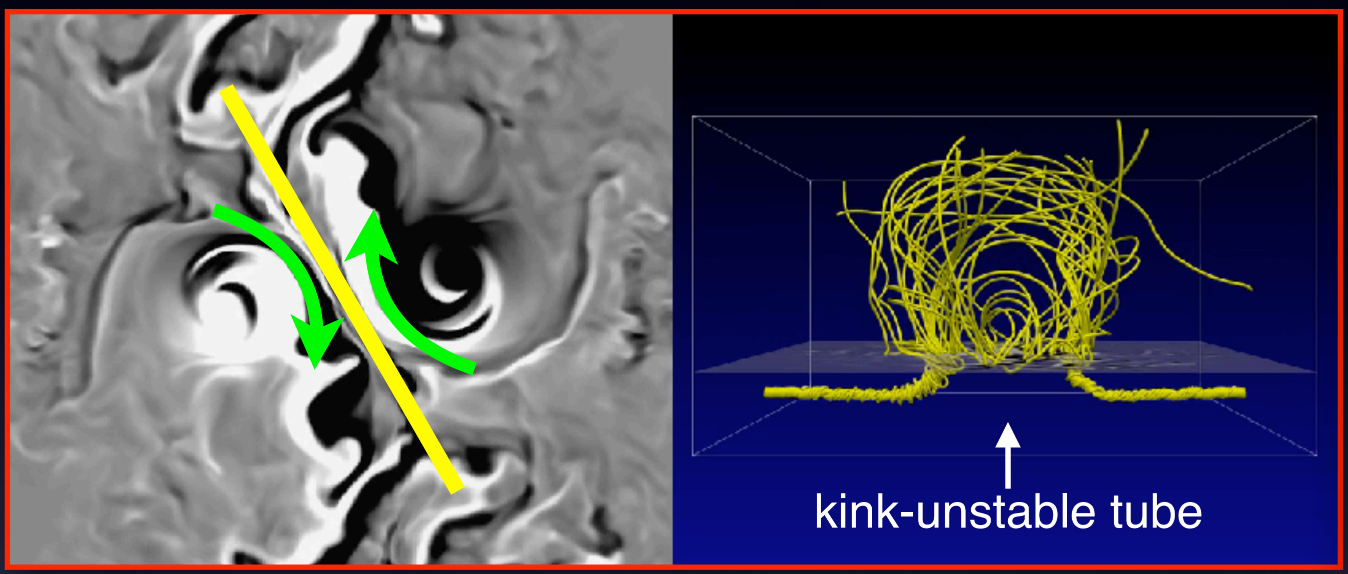

Spot-Satellite

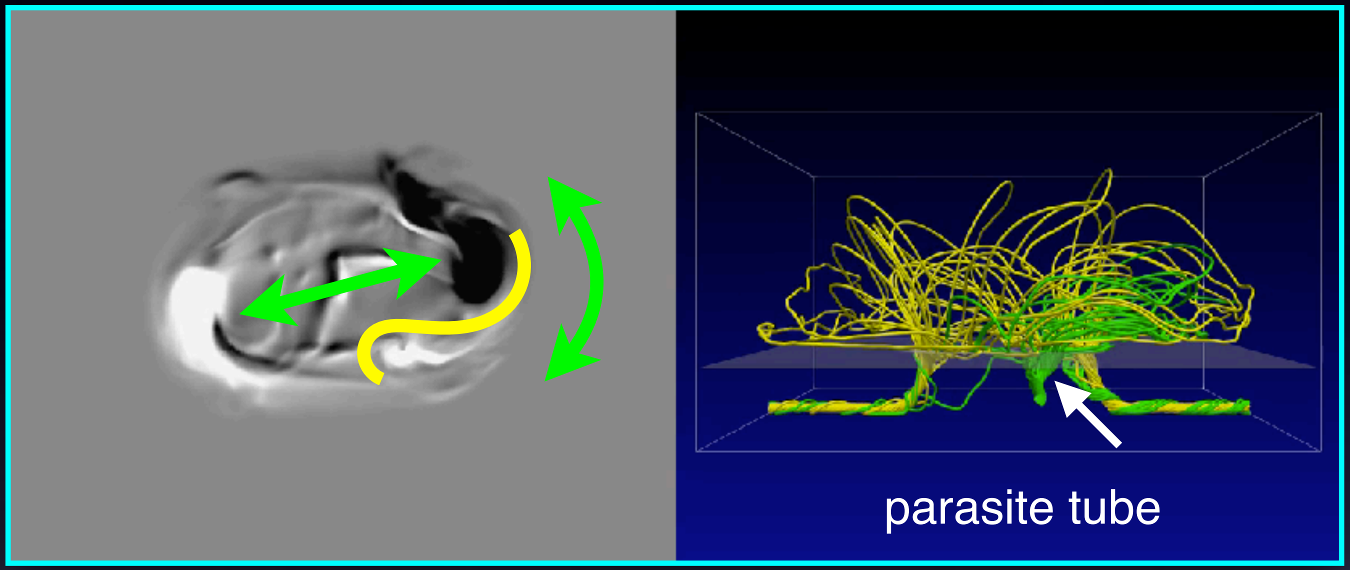

Quadrupole

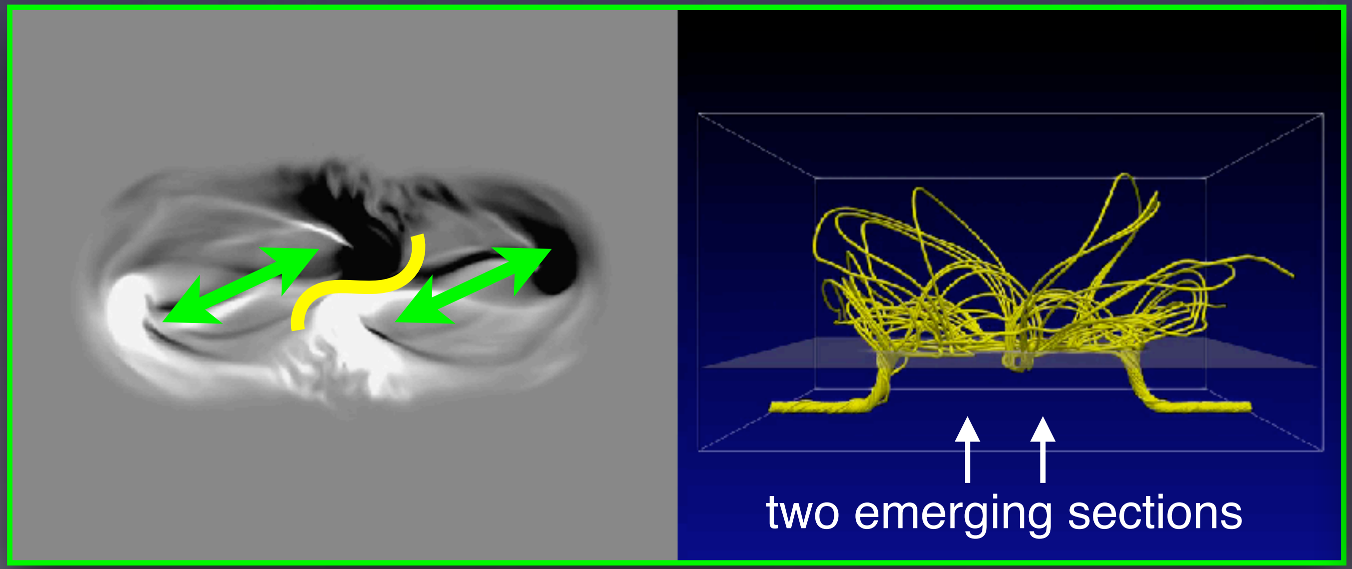

Inter-AR

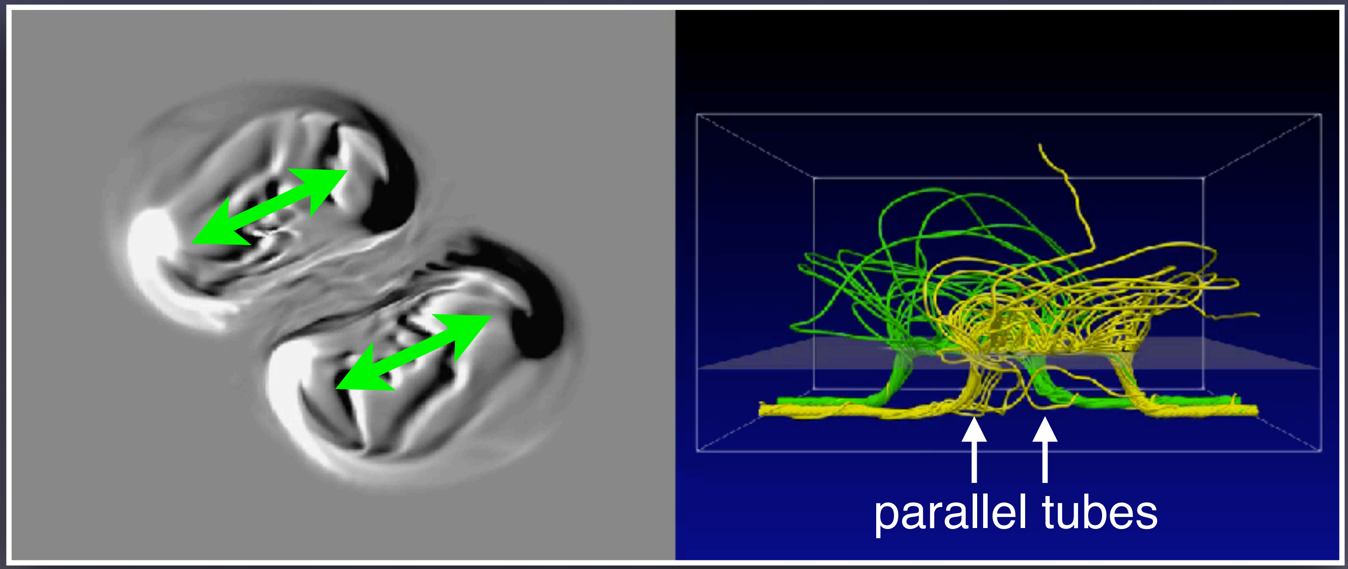

3. Modeling

- Formation of sheared PIL

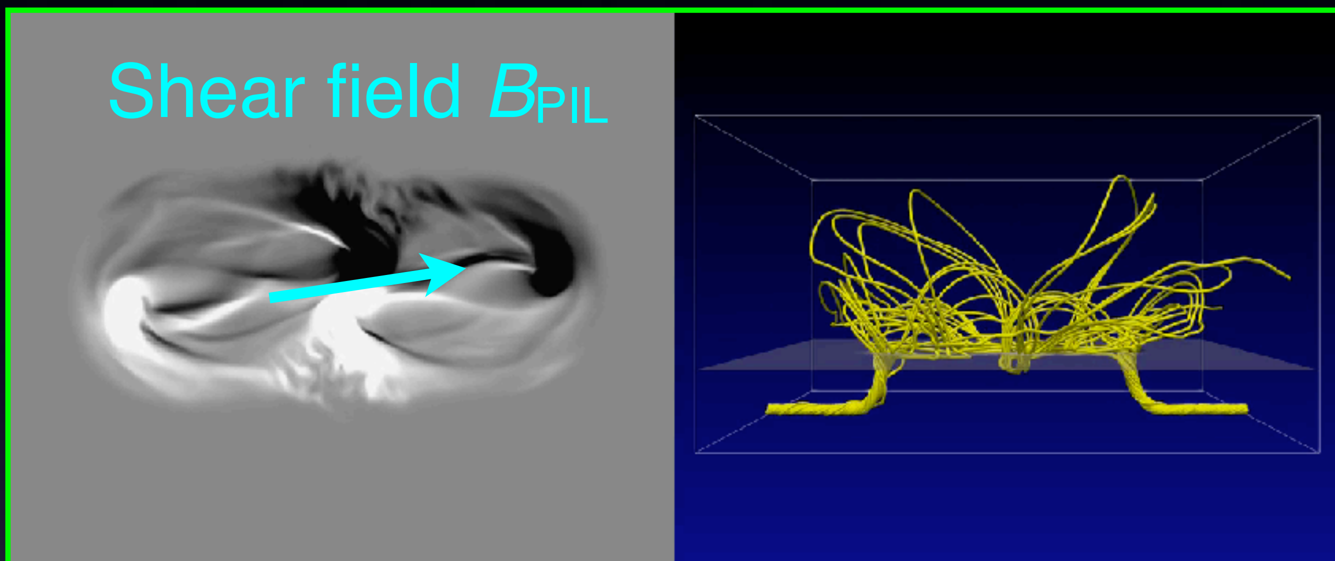

Quadrupole

$$\frac{\partial B_{\rm PIL}}{\partial t} = \underbrace{(\boldsymbol{B}\cdot\boldsymbol{\nabla})V_{\rm PIL}}_{\text{Stretching}} \underbrace{-(\boldsymbol{V}\cdot\boldsymbol{\nabla})B_{\rm PIL}}_{\text{Advection}}$$

$$\underbrace{-(\boldsymbol{\nabla}_{\rm h}\cdot\boldsymbol{V}_{\rm h})B_{\rm PIL}}_{\text{Compression (horizontal)}} \underbrace{-\frac{\partial V_z}{\partial z}B_{\rm PIL}}_{\text{Compression (vertical)}}$$

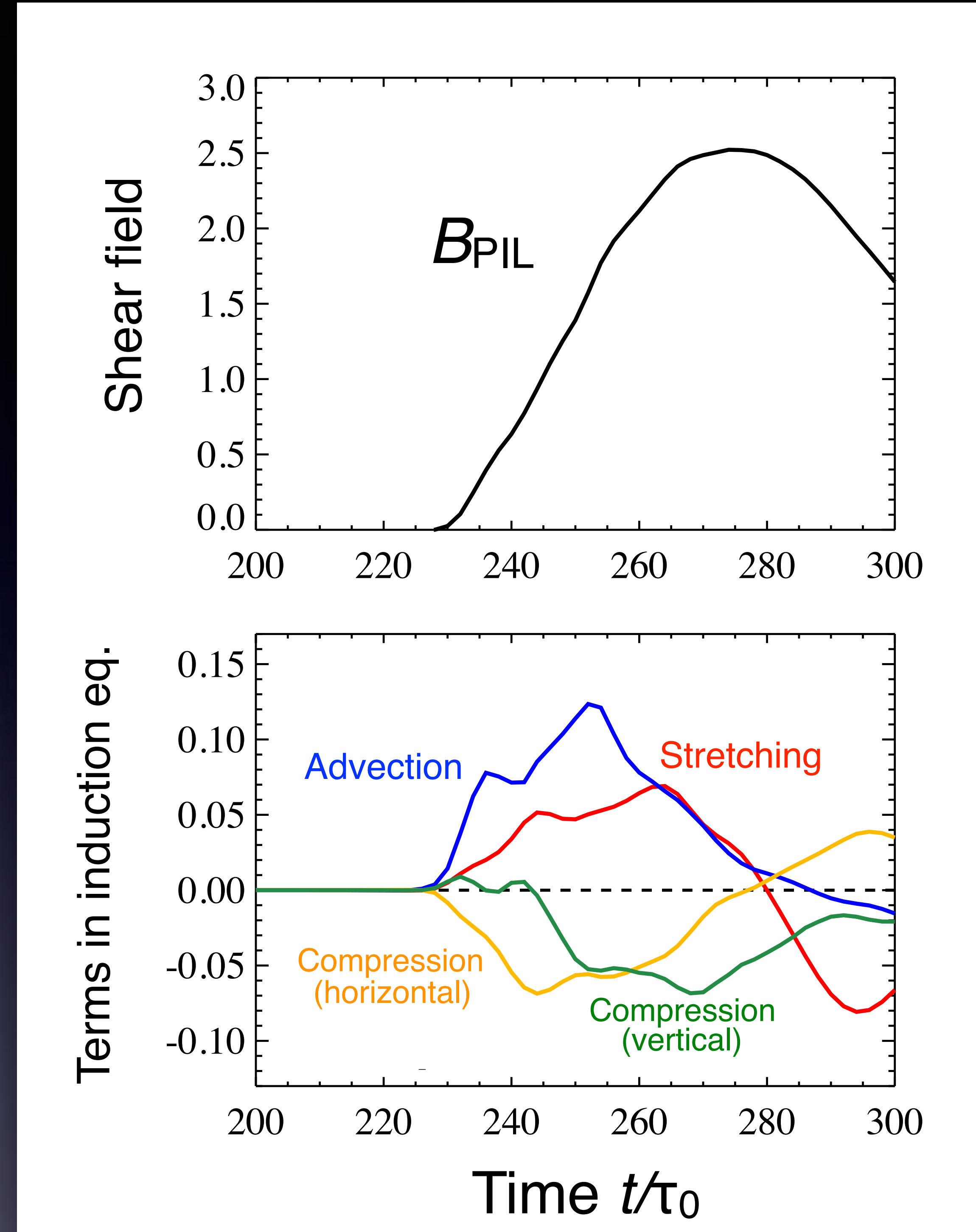

- Advection → Stretching → Compression
- Approaching spots transport the mag fields, then drift motion shears them, which are pressed later on.

3. Modeling

- Energy storage and flare prediction
  - SHARP parameters predict flares and CMEs well… WHY?
  - ↑ calculated from HMI vector magnetogram for each AR

GOOD ↑

Keyword	Description	Formula	F-Score
TOTUSJH	Total unsigned current helicity	$H_{c_{\text{total}}} \propto \sum \lvert B_z \cdot J_z \rvert$	3560
TOTBSQ	Total magnitude of Lorentz force	$F \propto \sum B^2$	3051
TOTPOT	Total photospheric magnetic free energy density	$\rho_{\text{tot}} \propto \sum \left(\boldsymbol{B}^{\text{Obs}} - \boldsymbol{B}^{\text{Pot}}\right)^2 dA$	2996
TOTUSJZ	Total unsigned vertical current	$J_{z_{\text{total}}} = \sum \lvert J_z \rvert dA$	2733
ABSNJZH	Absolute value of the net current helicity	$H_{c_{\text{abs}}} \propto \left\lvert \sum B_z \cdot J_z \right\rvert$	2618
SAVNCPP	Sum of the modulus of the net current per polarity	$J_{z_{\text{sum}}} \propto \left\lvert \sum^{B_z^+} J_z dA \right\rvert + \left\lvert \sum^{B_z^-} J_z dA \right\rvert$	2448
USFLUX	Total unsigned flux	$\Phi = \sum \lvert B_z \rvert dA$	2437
AREA_ACR	Area of strong field pixels in the active region	$\text{Area} = \sum \text{Pixels}$	2047
TOTFZ	Sum of z-component of Lorentz force	$F_z \propto \sum (B_x^2 + B_y^2 - B_z^2) dA$	1371
MEANPOT	Mean photospheric magnetic free energy	$\overline{\rho} \propto \frac{1}{N} \sum \left(\boldsymbol{B}^{\text{Obs}} - \boldsymbol{B}^{\text{Pot}}\right)^2$	1064
R_VALUE	Sum of flux near polarity inversion line	$\Phi = \sum \lvert B_{LoS} \rvert dA$ within R mask	1057
EPSZ	Sum of z-component of normalized Lorentz force	$\delta F_z \propto \frac{\sum (B_x^2 + B_y^2 - B_z^2)}{\sum B^2}$	864.1
SHRGT45	Fraction of Area with shear $> 45^\circ$	Area with shear $> 45^\circ$ / total area	740.8
MEANSHR	Mean shear angle	$\overline{\Gamma} = \frac{1}{N} \sum \arccos \left(\frac{\boldsymbol{B}^{\text{Obs}} \cdot \boldsymbol{B}^{\text{Pot}}}{\lvert B^{\text{Obs}} \rvert \lvert B^{\text{Pot}} \rvert} \right)$	727.9
MEANGAM	Mean angle of field from radial	$\overline{\gamma} = \frac{1}{N} \sum \arctan \left(\frac{B_h}{B_z} \right)$	573.3
MEANGBT	Mean gradient of total field	$\overline{\lvert \nabla B_{\text{tot}} \rvert} = \frac{1}{N} \sum \sqrt{\left(\frac{\partial B}{\partial x}\right)^2 + \left(\frac{\partial B}{\partial y}\right)^2}$	192.3
MEANGBZ	Mean gradient of vertical field	$\overline{\lvert \nabla B_z \rvert} = \frac{1}{N} \sum \sqrt{\left(\frac{\partial B_z}{\partial x}\right)^2 + \left(\frac{\partial B_z}{\partial y}\right)^2}$	88.40
MEANGBH	Mean gradient of horizontal field	$\overline{\lvert \nabla B_h \rvert} = \frac{1}{N} \sum \sqrt{\left(\frac{\partial B_h}{\partial x}\right)^2 + \left(\frac{\partial B_h}{\partial y}\right)^2}$	79.40
MEANJZH	Mean current helicity (B_z contribution)	$\overline{H_c} \propto \frac{1}{N} \sum B_z \cdot J_z$	46.73
TOTFY	Sum of y-component of Lorentz force	$F_y \propto \sum B_y B_z dA$	28.92
MEANJZD	Mean vertical current density	$\overline{J_z} \propto \frac{1}{N} \sum \left(\frac{\partial B_y}{\partial x} - \frac{\partial B_x}{\partial y} \right)$	17.44
MEANALP	Mean characteristic twist parameter, α	$\alpha_{\text{total}} \propto \frac{\sum J_z \cdot B_z}{\sum B_z^2}$	10.41
TOTFX	Sum of x-component of Lorentz force	$F_x \propto -\sum B_x B_z dA$	6.147
EPSY	Sum of y-component of normalized Lorentz force	$\delta F_y \propto \frac{-\sum B_y B_z}{\sum B^2}$	0.647
EPSX	Sum of x-component of normalized Lorentz force	$\delta F_x \propto \frac{\sum B_x B_z}{\sum B^2}$	0.366

BAD ↓

[Bobra & Couvidat 2015; also Bobra & Ilonidis 2016, Nishizuka+ 2017]

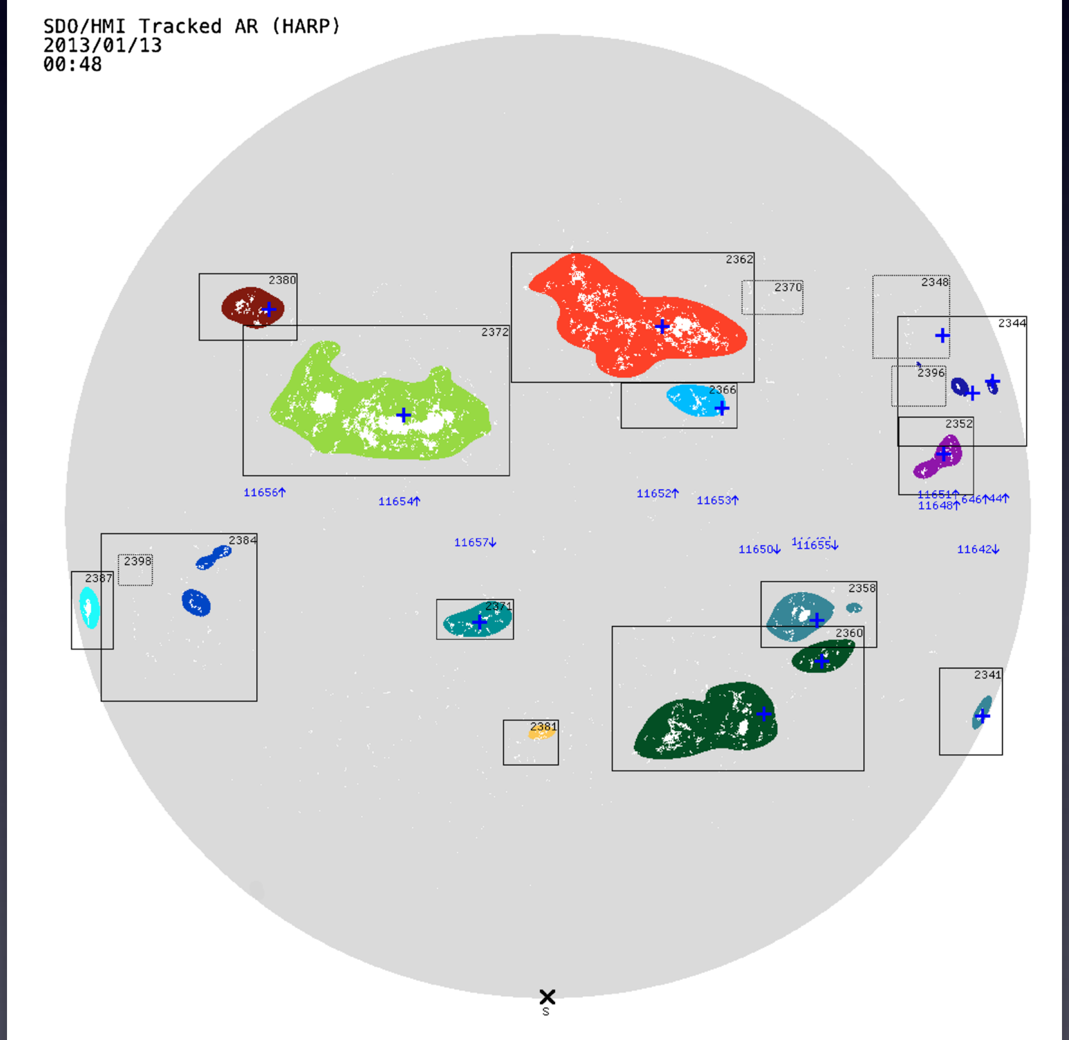

Auto-detection of ARs [Bobra et al. 2014]

3. Modeling

- Energy storage and flare prediction
  - SHARP parameters predict flares and CMEs well… WHY?
  - ↑ calculated from HMI vector magnetogram for each AR

GOOD ↑

BAD ↓

Keyword	Description	Formula	*F*-Score
TOTUSJH	Total unsigned current helicity	$H_{c_{\text{total}}} \propto \sum \lvert B_z \cdot J_z \rvert$	3560
TOTBSQ	Total magnitude of Lorentz force	$F \propto \sum B^2$	3051
TOTPOT	Total photospheric magnetic free energy density	$\rho_{\text{tot}} \propto \sum \left(\boldsymbol{B}^{\text{Obs}} - \boldsymbol{B}^{\text{Pot}}\right)^2 dA$	2996
TOTUSJZ	Total unsigned vertical current	$J_{z_{\text{total}}} = \sum \lvert J_z \rvert dA$	2733
ABSNJZH	Absolute value of the net current helicity	$H_{c_{\text{abs}}} \propto \left\lvert \sum B_z \cdot J_z \right\rvert$	2618
SAVNCPP	Sum of the modulus of the net current per polarity	$J_{z_{\text{sum}}} \propto \left\lvert \sum^{B_z^+} J_z dA \right\rvert + \left\lvert \sum^{B_z^-} J_z dA \right\rvert$	2448
USFLUX	Total unsigned flux	$\Phi = \sum \lvert B_z \rvert dA$	2437
AREA_ACR	Area of strong field pixels in the active region	Area $= \sum$ Pixels	2047
TOTFZ	Sum of z-component of Lorentz force	$F_z \propto \sum (B_x^2 + B_y^2 - B_z^2) dA$	1371
MEANPOT	Mean photospheric magnetic free energy	$\overline{\rho} \propto \frac{1}{N} \sum \left(\boldsymbol{B}^{\text{Obs}} - \boldsymbol{B}^{\text{Pot}}\right)^2$	1064
R_VALUE	Sum of flux near polarity inversion line	$\Phi = \sum \lvert B_{LoS} \rvert dA$ within R mask	1057
EPSZ	Sum of z-component of normalized Lorentz force	$\delta F_z \propto \frac{\sum (B_x^2 + B_y^2 - B_z^2)}{\sum B^2}$	864.1
SHRGT45	Fraction of Area with shear $> 45^\circ$	Area with shear $> 45^\circ$ / total area	740.8
MEANSHR	Mean shear angle	$\overline{\Gamma} = \frac{1}{N} \sum \arccos \left(\frac{\boldsymbol{B}^{\text{Obs}} \cdot \boldsymbol{B}^{\text{Pot}}}{\lvert B^{\text{Obs}} \rvert \lvert B^{\text{Pot}} \rvert} \right)$	727.9
MEANGAM	Mean angle of field from radial	$\overline{\gamma} = \frac{1}{N} \sum \arctan \left(\frac{B_h}{B_z} \right)$	573.3
MEANGBT	Mean gradient of total field	$\overline{\lvert \nabla B_{\text{tot}} \rvert} = \frac{1}{N} \sum \sqrt{\left(\frac{\partial B}{\partial x}\right)^2 + \left(\frac{\partial B}{\partial y}\right)^2}$	192.3
MEANGBZ	Mean gradient of vertical field	$\overline{\lvert \nabla B_z \rvert} = \frac{1}{N} \sum \sqrt{\left(\frac{\partial B_z}{\partial x}\right)^2 + \left(\frac{\partial B_z}{\partial y}\right)^2}$	88.40
MEANGBH	Mean gradient of horizontal field	$\overline{\lvert \nabla B_h \rvert} = \frac{1}{N} \sum \sqrt{\left(\frac{\partial B_h}{\partial x}\right)^2 + \left(\frac{\partial B_h}{\partial y}\right)^2}$	79.40
MEANJZH	Mean current helicity (B_z contribution)	$\overline{H_c} \propto \frac{1}{N} \sum B_z \cdot J_z$	46.73
TOTFY	Sum of y-component of Lorentz force	$F_y \propto \sum B_y B_z dA$	28.92
MEANJZD	Mean vertical current density	$\overline{J_z} \propto \frac{1}{N} \sum \left(\frac{\partial B_y}{\partial x} - \frac{\partial B_x}{\partial y} \right)$	17.44
MEANALP	Mean characteristic twist parameter, α	$\alpha_{\text{total}} \propto \frac{\sum J_z \cdot B_z}{\sum B_z^2}$	10.4[illegible]
TOTFX	Sum of x-component of Lorentz force	$F_x \propto -\sum B_x B_z dA$	[illegible].147
EPSY	Sum of y-component of normalized Lorentz force	$\delta F_y \propto \frac{-\sum B_y B_z}{\sum B^2}$	0.647
EPSX	Sum of x-component of normalized Lorentz force	$\delta F_x \propto \frac{\sum B_x B_z}{\sum B^2}$	0.366

[Bobra & Couvidat 2015; also Bobra & Ilonidis 2016, Nishizuka+ 2017]

Total unsigned current helicity

$$H_{C\text{total}} \propto \sum \lvert B_z \cdot J_z \rvert$$

Total photospheric mag free energy

$$\rho_{\text{tot}} \propto \sum (\boldsymbol{B}^{\text{Obs}} - \boldsymbol{B}^{\text{Pot}})^2 dA$$

Sum of x-comp. of norm. Lorentz force

$$\delta F_x \propto \sum B_x B_z dA \,/\, \sum B^2$$

3. Modeling

- Energy storage and flare prediction

Free mag. energy in the corona

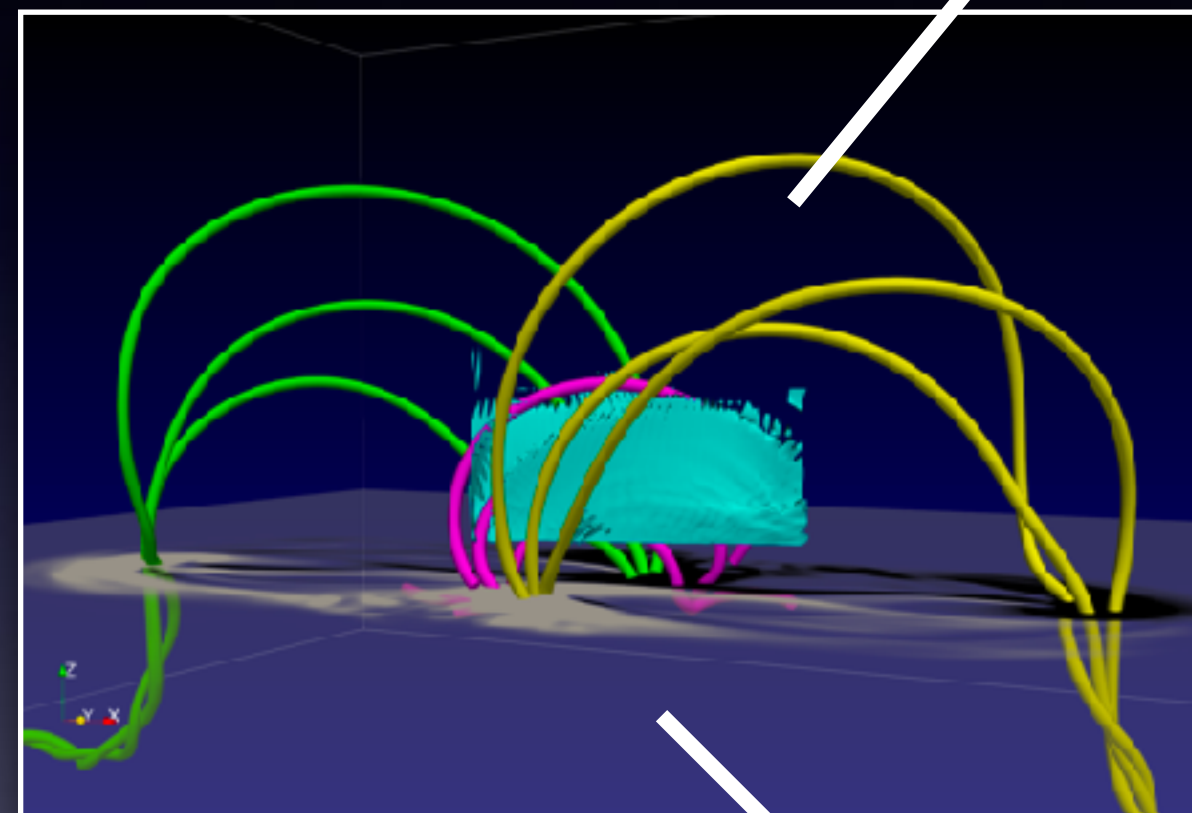

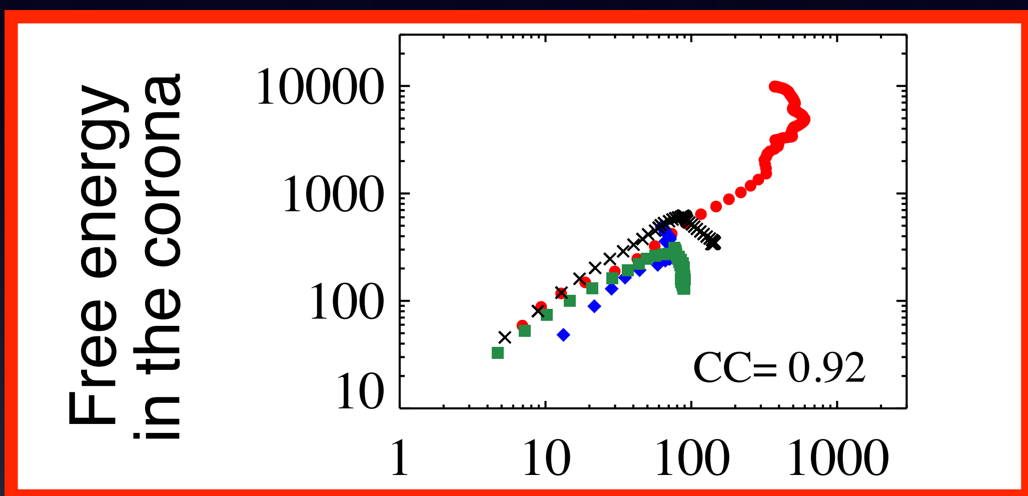

SHARP parameters in the photosphere

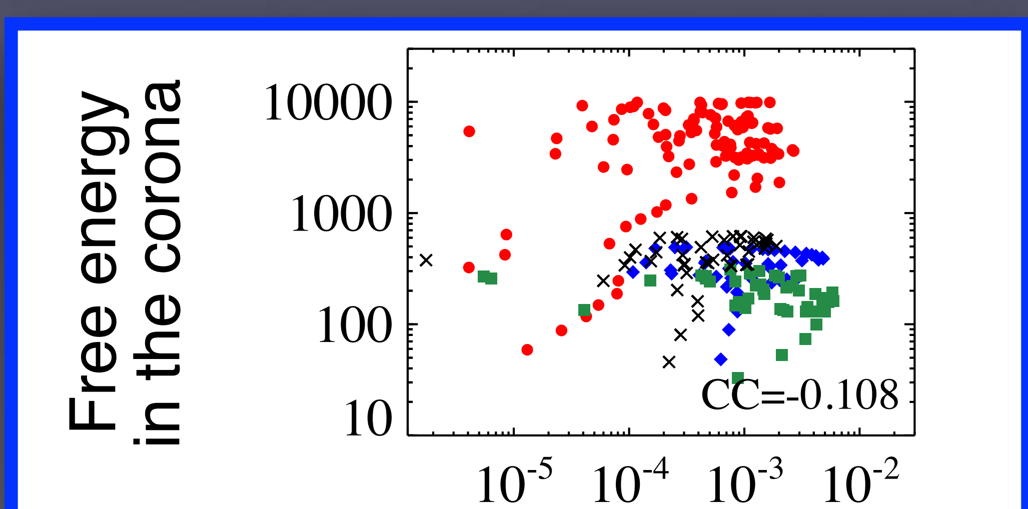

3. Modeling

- Energy storage and flare prediction

Total unsigned current helicity

$$H_{C\text{total}} \propto \sum |B_z \cdot J_z|$$

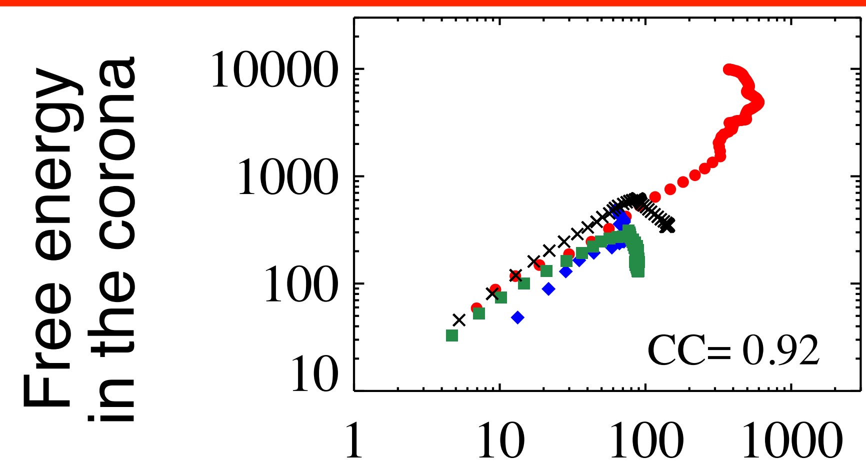

Sum of x-comp. of norm. Lorentz force

$$\delta F_x \propto \sum B_x B_z dA \,/ \sum B^2$$

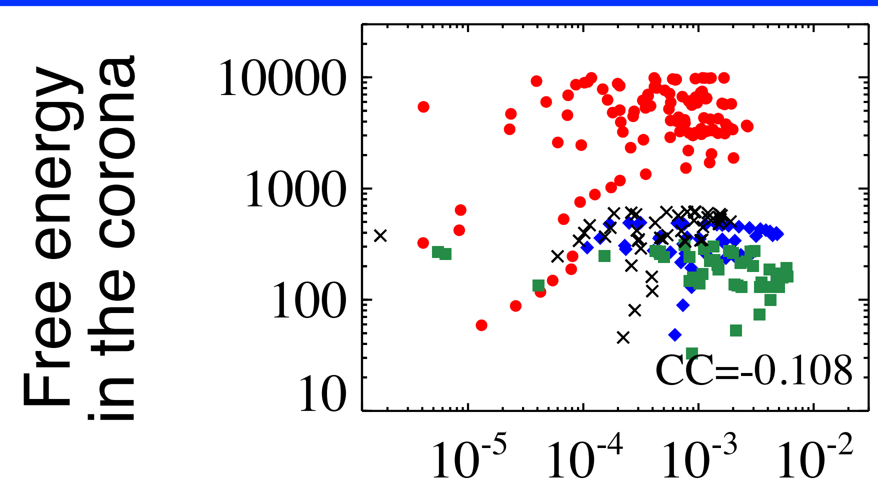

- Flare-predictive parameters
  → Strong correlation with free energy
- Non-predictive parameters
  → Almost NO correlation

SHARP parameters in the photosphere can measure the free energy in the corona and thus predict flares accurately.

4. Summary

- Observation
  - All ≥M5.0-class flares for 6 years → 51 flares from 29 ARs
  - >80% contain δ-spots, ~15% violate Hale's rule
  - Categorization into four types, and many more…

  Toriumi et al. 2017

- Modeling
  - FE simulations → δ-spots with sheared PILs
  - PIL created by advection → stretching → compression
  - Flare-predictive SHARP parameters reflect stored free energy

  Toriumi & Takasao 2017

↓

Complexity and interaction of subsurface emerging flux produce flaring ARs

Movie courtesy of M. DeRosa

Thank you for your attention!